(NASA-TM-82077) THE PRESIDENT'S DAY CYCLONE 17-19 FEBRUARY 1979: AN ANALYSIS OF JET STREAK INTERACTIONS PRIOR TO CYCLOGENESIS (NASA) 67 p HC A04/MF A01 CSCL 04B

N81-20658

Unclas
G3/47 18833

NASA

Technical Memorandum 82077

THE PRESIDENT'S DAY CYCLONE 17-19 FEBRUARY 1979: AN ANALYSIS OF JET STREAK INTERACTIONS PRIOR TO CYCLOGENESIS

L. W. Uccellini, P. J. Kocin and
C. H. Wash

JANUARY 1981

National Aeronautics and
Space Administration

Goddard Space Flight Center
Greenbelt, Maryland 20771

TM 82077

THE PRESIDENT'S DAY CYCLONE 17-19 FEBRUARY 1979: AN ANALYSIS OF JET STREAK INTERACTIONS PRIOR TO CYCLOGENESIS

Louis W. Uccellini
NASA/Goddard Space Flight Center
Laboratory for Atmospheric Sciences
Greenbelt, Maryland 20771

Paul J. Kocin
NASA/Goddard Space Flight Center
Laboratory for Atmospheric Sciences
Greenbelt, Maryland 20771

Carlyle H. Wash
Space Science and Engineering Center
University of Wisconsin
Madison, Wisconsin

January 1981

NATIONAL AERONAUTICS AND SPACE ADMINISTRATION
GODDARD SPACE FLIGHT CENTER
Greenbelt, Maryland

THE PRESIDENT'S DAY CYCLONE 17-19 FEBRUARY 1979: AN ANALYSIS OF JET STREAK INTERACTIONS PRIOR TO CYCLOGENESIS

Louis W. Uccellini
NASA/Goddard Space Flight Center
Laboratory for Atmospheric Sciences
Greenbelt, Maryland 20771

Paul J. Kocin
NASA/Goddard Space Flight Center
Laboratory for Atmospheric Sciences
Greenbelt, Maryland 20771

Carlyle H. Wash
Space Science and Engineering Center
University of Wisconsin
Madison, Wisconsin

ABSTRACT

An analysis is presented of the President's Day cyclone, which produced record breaking snowfall along the East Coast of the United States on February 18-19, 1979. Conventional radiosonde data, SMS GOES infrared imagery and LFM-II model diagnostics are utilized in the analysis, which focuses on the interaction of upper and lower tropospheric jet streaks prior to cyclogenesis. The analysis reveals that a series of complex scale interactive processes is responsible for the development of the intense cyclone. Specific findings include: (1) two distinct "systems," as defined by separate cloud masses and distinct areas of converging isallobaric winds, are responsible for the heavy snow, (2) the development of a low level jet (LLJ) by 1200 GMT 18 February along the southeast Atlantic Coast is linked to a significantly supergeostrophic subtropical jet (STJ) and the damming of cold air east of the Appalachian Mountains through isallobaric forcing, (3) the isallobaric forcing of the LLJ played a dual role in generating mesoscale regions of heavy

snow through accelerated moisture transport into the region of heaviest precipitation and enhanced low level convergence associated with the isallobaric wind, and (4) the LFM-II simulation suffers from an inability to predict the development of the LLJ along the East Coast prior to and during cyclogenesis. It appears that the LFM-II predicts a direct circulation along the coast rather than the observed indirect circulation, a failure which has serious implications for the ability to predict the rapid cyclogenesis and the heavy precipitation that characterize this storm.

It appears that the transverse circulations associated with jet streaks and coastal fronts act to produce a more favorable region for cyclogenesis and to generate mesoscale areas of heavy snowfall. These types of processes have been discussed for spring convective storm systems (Uccellini and Johnson, 1979). However, the pre-cyclogenetic environment, with rapidly accelerating upper tropospheric flow, is far more complicated than the simplified view of jet streak adjustments presented by Uccellini and Johnson for the case involving straight jet flow in a non-cyclogenetic period.

CONTENTS

LIST OF FIGURES

LIST OF FIGURES (Continued)

THE PRESIDENT'S DAY CYCLONE 17–19 FEBRUARY 1979: AN ANALYSIS OF JET STREAK INTERACTIONS PRIOR TO CYCLOGENESIS

1. INTRODUCTION

On 18–19 February 1979, an intense cyclone developed along the Middle Atlantic Coast. The storm produced 45 to 60cm of snow from Virginia to southern New Jersey, including the heaviest snowfall in Washington, D.C. in over 50 years (Foster and Leffler, 1979). Bosart (1980) has presented an analysis of this intense cyclone (known as the President's Day cyclone, emphasizing the coastal frontogenesis on the 18th of February which preceded cyclogenesis and the apparent contribution of boundary layer processes and diabatic heating to the rapid vortex development which occurred on the 19th of February.

Scientists at the National Meteorological Center (NMC) are studying the President's Day storm and conducting numerical experiments to determine the reasons for the failure of the operational Limited Area Fine Mesh (LFM–II) model to accurately forecast the cyclogenesis and heavy snowfall. The Global Atmospheric Research Program (GARP) group of the Goddard Modeling and Simulation Facility (GMSF) is also actively studying the President's Day storm as it occurred during one of the First GARP Global Experiment (FGGE) observing periods. Therefore, the President's Day storm provides a unique opportunity to examine East Coast cyclogenesis with FGGE global data sets.

The purposes of this technical report are: (1) to document the evolution of the subsynoptic scale mass and momentum fields prior to and during the period of rapid development of the President's Day cyclone utilizing conventional data and SMS-GOES imagery, (2) to discuss the interaction between upper and lower tropospheric jet streaks that occurred prior to the onset of cyclogenesis, (3) to discuss the possible effects of terrain modified airflow within the pre-cyclogenesis environment, and (4) to explore possible deficiencies in the LFM–II initial wind

fields that could have been responsible, in part, for the poor numerical forecast. In Section 2 of this report, a synoptic analysis is presented to provide a general overview of the President's Day storm. A more detailed analysis is presented in Section 3, which focuses on the interaction between upper and lower level jets prior to cyclogenesis. The damming of cold air against the eastern slopes of the Appalachian Mountains and its influence upon the pre-cyclogenesis environment are also examined in Section 3. Section 4 briefly discusses the LFM-II model simulations initialized prior to cyclogenesis (0000 GMT 18 February, and 1200 GMT 18 February). Section 5 summarizes the results of the study and presents questions for future research.

2. CASE STUDY, A SYNOPTIC OVERVIEW

Introduction

Figures 1 through 5, which depict the National Weather Service (NWS) surface, 850mb and 300mb analyses for 1200 GMT 17 February 1979 through 1200 GMT 19 February 1979, provide a synoptic overview of the period prior to and during the cyclogenesis, a period during which significant mass and momentum adjustments occurred over the entire eastern half of the United States.

At 1200 GMT 17 February, a massive high pressure system centered over the Great Lakes region (Figure 1C) was marked by extremely cold air with record low surface temperatures reported from southern Canada to the mid-Atlantic states. Light snow had already developed within the southerly return flow over the Great Plains in response to an upper level wave propagating from the southwest toward the southern Great Plains (Figure 1A). The 300mb map also reveals two distinct jet streaks: a polar jet located off the East Coast and a subtropical jet directed from Mexico toward northern Arkansas.

By 0000 GMT 18 February (Figure 2), the large anticyclone was still centered over the Great Lakes region with a portion of the high pressure system extending down the East Coast evident at both the surface (Figure 2C) and the 850mb (Figure 2B) levels. The snow and sleet in the

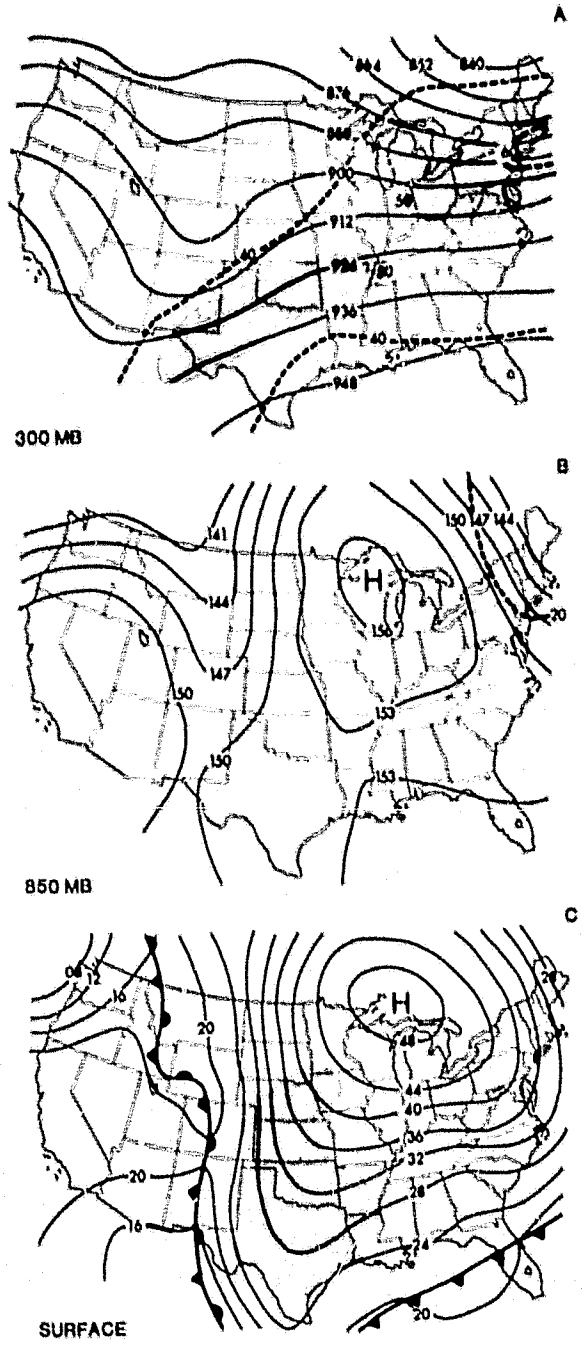

Figure 1. Isobaric and surface analyses for 1200 GMT 17 February 1979. (A) 300 mb geopotential height (solid, 900 = 9000 m) and isotach (dashed, ms^{-1}; shaded region represents velocities between 50 ms^{-1} and 60 ms^{-1}). (B) 850 mb geopotential height (solid, 150 = 1500 m) and isotach (dashed, ms^{-1}). (C) Surface isobars (solid, 40 = 1040 millibars), precipitation (shaded).

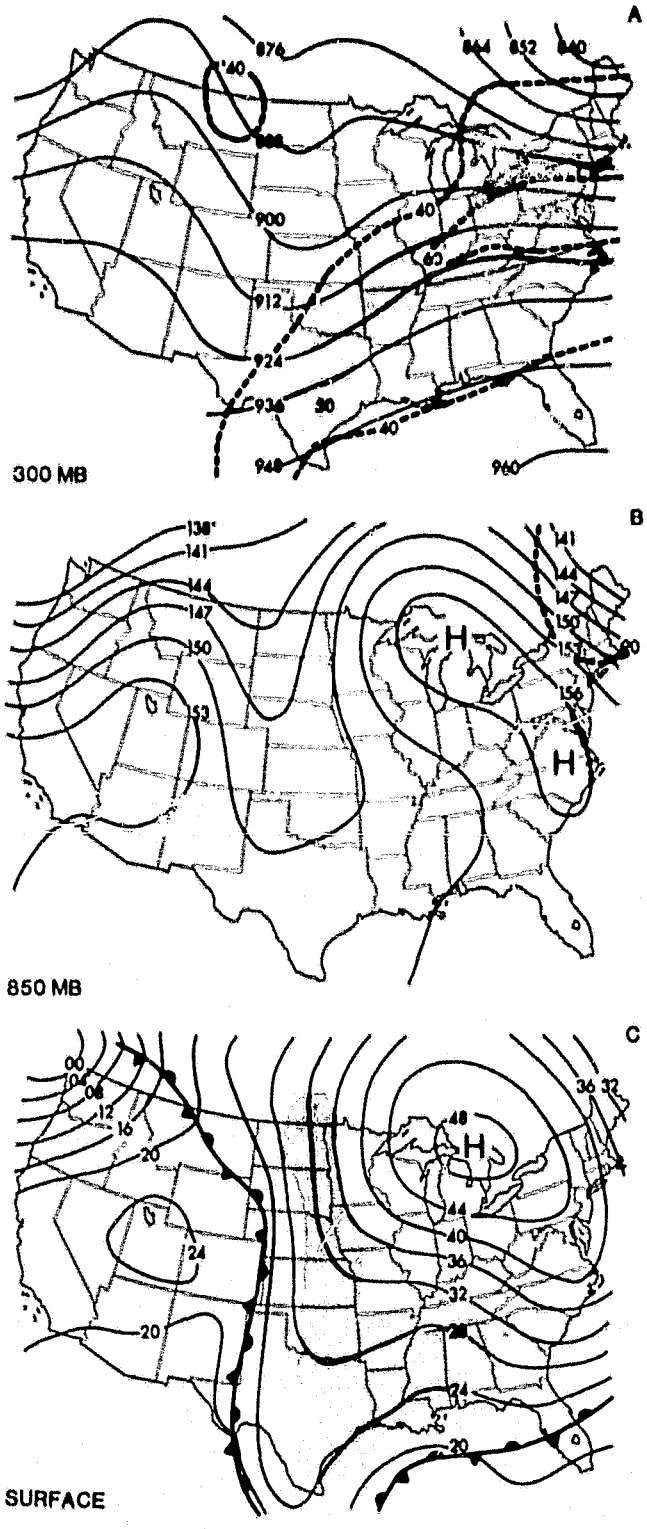

Figure 2. Isobaric and surface analyses for 0000 GMT 18 February 1979. See caption for Figure 1 for additional details.

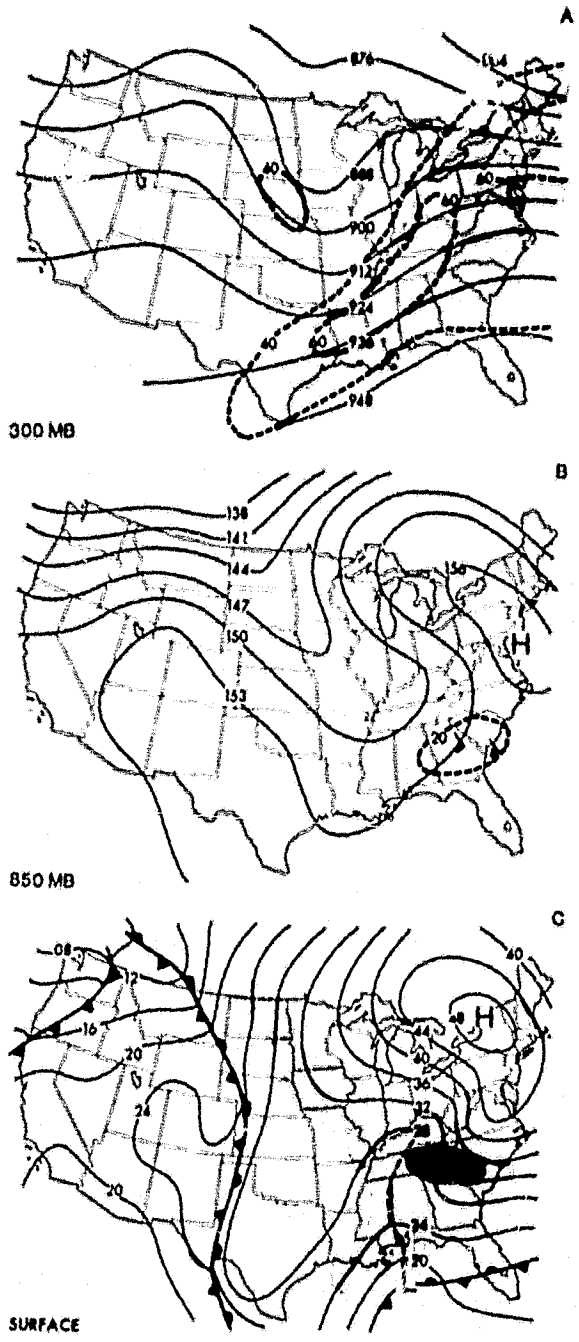

Figure 3. Isobaric and surface analyses for 1200 GMT 18 February 1979. (B) Wind barbs represent largest measured velocities (each barb denotes a 10 ms^{-1} velocity; a half barb denotes a 5 ms^{-1} velocity). (C) Heavy shading denotes moderate to heavy precipitation. Dashed line indicates inverted trough. See Figure 1 caption for additional details.

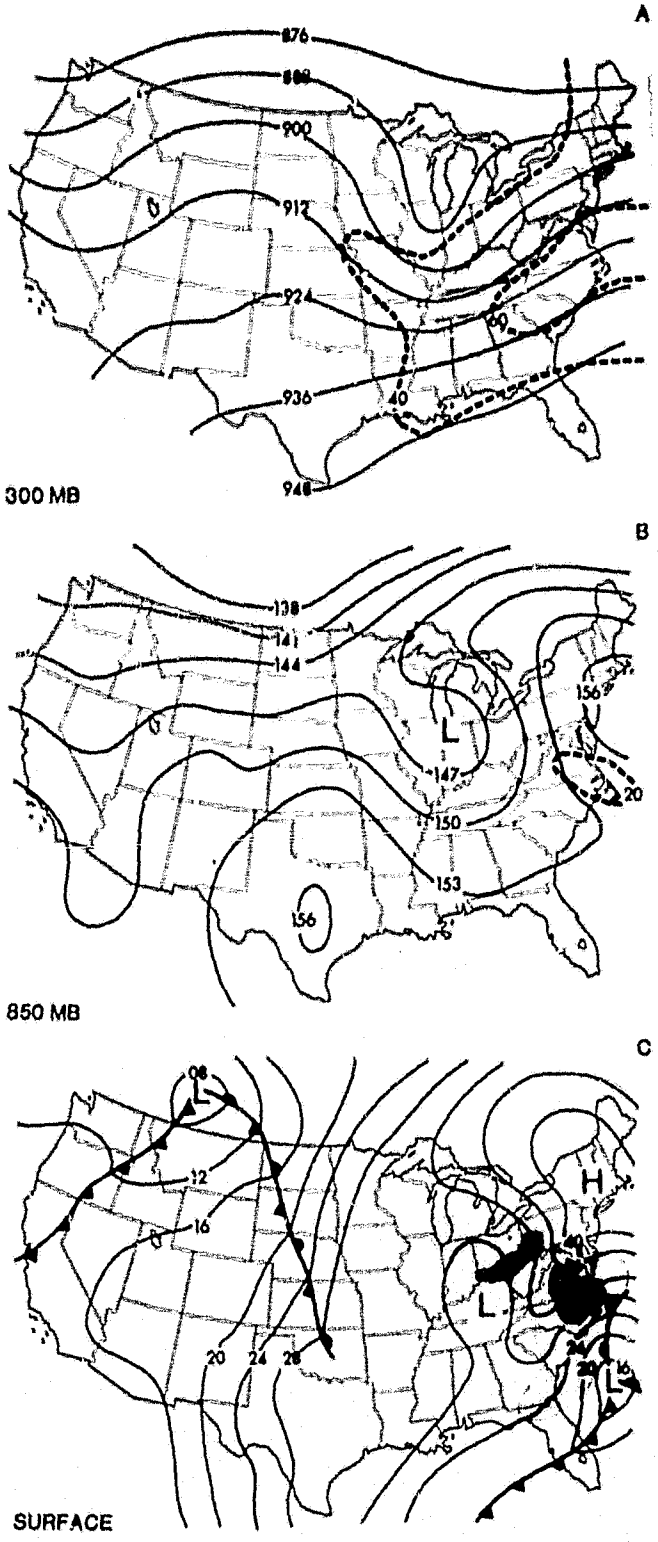

Figure 4. Isobaric and surface analyses for 0000 GMT 19 February 1979. See Figure 1 and Figure 3 captions for additional details.

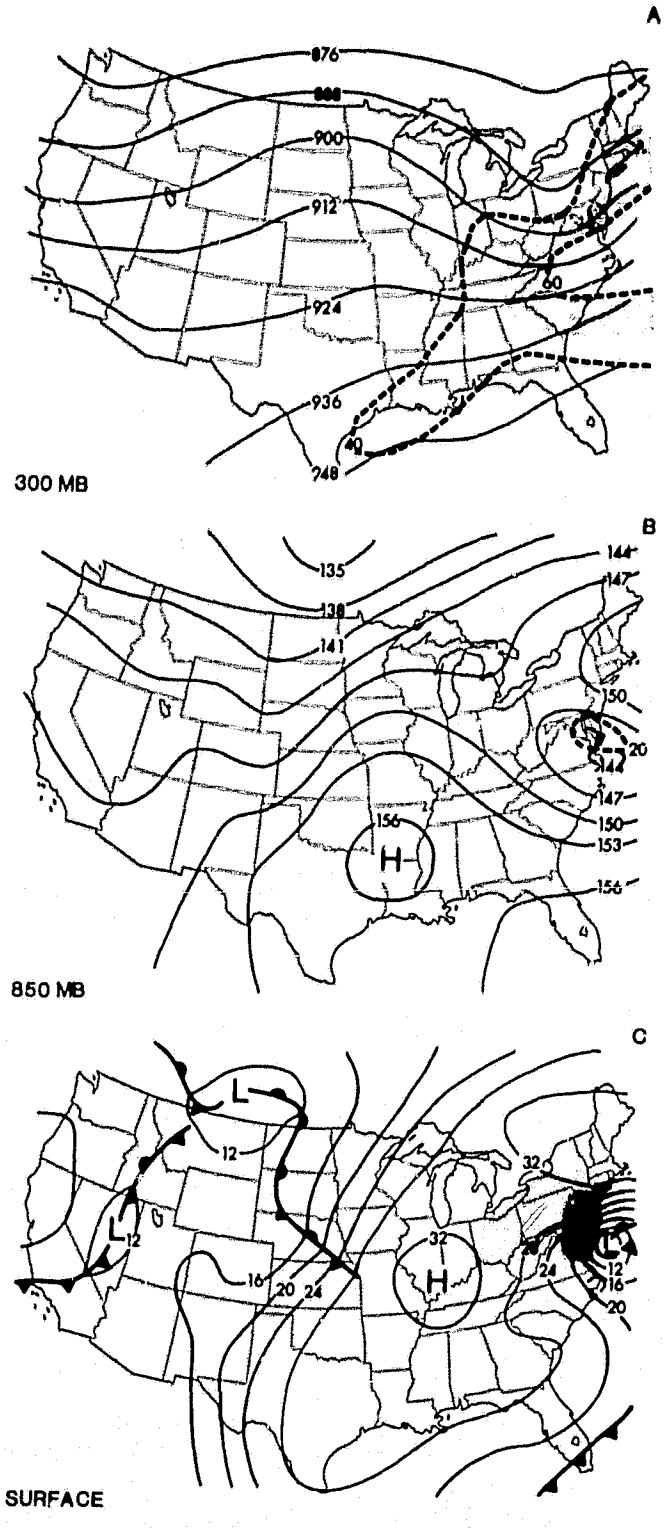

Figure 5. Isobaric and surface analyses for 1200 GMT 19 February 1979. See Figure 1 and Figure 3 captions for additional details.

southern United States continued moving toward the east as the surface and 850mb maps provide the first indication of an inverted trough extending northward from the Gulf of Mexico. The jet streaks analyzed on the 300mb surface, with maximum wind speeds generally between 50 and 60ms^{-1}, appeared to merge as the wave in the Great Plains continued to propagate east.

By 1200 GMT 18 February (Figure 3), several important changes in the mass and wind field occurred within the entire troposphere. A surface low began developing along the Gulf Coast with a well defined inverted trough extending into the Ohio Valley. Moderate to heavy snow was now reported within the Tennessee Valley and southern Appalachians and a broad area of light snow extended into the midwestern states (Figure 3C). Significant accelerations in the 850 and 300mb wind fields are clearly evident. At 850mb, winds over the Southeast increased from 5ms^{-1} at 0000 GMT to greater than 25ms^{-1} by 1200 GMT 18 February. The low level winds were noticeably ageostrophic and directed across the 850mb geopotential height contours at an angle approaching 90° (Figure 3B). The 300mb winds from Texas to Kentucky increased 15ms^{-1} to a maximum value nearing 65ms^{-1}.

By 0000 GMT 19 February, a surface low progressed eastward to a point off the Georgia coast with a second weaker low located in the Ohio Valley (Figure 4C). Strong surface ridging persisted along the Atlantic coastal region providing evidence of the entrenchment of extremely cold air east of the mountains.[1] The coastal front that developed along the East Coast (Bosart, 1980) is clearly evident on the synoptic analysis. Two separate areas of moderate snow are observed with the southernmost area being the dominant feature at this time. The 850mb analysis (Figure 4B) indicates that the low level wind maximum progressed northeastward along the coast and that the 850mb wave over the Ohio Valley amplified. The increased amplitude of the Ohio

[1]Several stations (including Richmond, Virginia) had maximum temperatures on the 18th of February that were lower than previous minimum temperature records.

Valley trough is also evident at the 300mb level (Figure 4A). However, the maximum winds at 300mb are still located along the coast to the east of the trough line.

By 1200 GMT 19 February (Figure 5), cyclogenesis was in progress along the Virginia coast with heavy snow extending from northern Virginia to extreme southeastern New York (Figure 5C). Bosart's (1980) analysis indicates that the coastal front was still apparent in eastern Maryland, providing the enhanced low level convergence that maximized the snowfall rate in the Washington, D.C. to Wilmington, Delaware corridor.[2] The 850mb map (Figure 5B) reveals an intense circulation off the East Coast which reflects the eastward shift and amplification of the wave previously located in Ohio. The 300mb map (Figure 5A) reveals that the upper tropospheric wave translated east, but did not amplify at this time. In fact, it appears that the amplitude of the 300mb wave decreased as the lower tropospheric cyclonic vortex rapidly developed. However, the maximum winds at the 300mb level were now located at the base of the trough, such that the cyclonic shears and curvature vorticity coincided for the first time in the course of the storm's evolution. This factor is probably important for increasing the vorticity, vorticity advection and upper level divergence that could enhance the cyclogenetic process observed during this period.

SMS-GOES Infrared Imagery

Interesting aspects of the President's Day cyclone include the rapid cyclogenesis, rapid vortex development and the uncertainty regarding the cyclone's movement between 0000 GMT and 1200 GMT 19 February. A review of the 3-hourly NWS surface maps and Bosart's analysis indicate that a surface low moved up the coast. However, the 300mb wave and 850mb trough appear to actually move east from the Ohio Valley region during the critical period immediately prior to

[2]Snowfall rates approached $12 cm h^{-1}$ just north of Washington, D.C. during this period (Foster and Leffler, 1979).

cyclogenesis. It therefore appears that a complex interaction between separate "systems" played an important role in the development of the President's Day cyclone.

An inspection of the SMS-GOES infrared imagery reveals that two separate precipitation regimes produced the heavy snows on the 18th and 19th of February 1979. A sequence of 6-hourly images (Figure 6) shows an extensive cloud shield over the Southeast at 1200 GMT 18 February, which had been rapidly expanding up to this time and subsequently moved east producing the heavy snows in Tennessee, the Carolinas and southern Virginia. The heaviest snow did not occur under the coldest cirrus cloud tops. Rather, they occurred along the upstream edge of the cloud domain, especially within the southern portion. Between 1200 GMT 18 February and 1200 GMT 19 February, this cloud area appeared to weaken in intensity, shrink in size and move toward the east, and was located off the East Coast as cyclogenesis commenced between 0000 GMT and 0600 GMT.

At 1200 GMT 18 February, a second, less distinct area of clouds displaying a vortical form was located over the northern Midwest. This second area of clouds is clearly associated with the upper level wave observed over the northern Midwest (Figure 3A). The cloud area rapidly intensified and expanded as it moved toward the East Coast between 0000 GMT and 1200 GMT 19 February. The rapid intensification and expansion of the eastward propagating cloud mass produced up to 40cm of snow in western Pennsylvania and the heavy snow in the Washington, D.C. to New York City corridor.

An inspection of the hourly sequence of infrared imagery (Figure 7) reveals that the rapid intensification and expansion of the second cloud area coincided with the rapid cyclogenesis off the North Carolina-Virginia coast (which commenced at 0300-0600 GMT 19 February) and appears to be associated with the Ohio Valley wave propagating rapidly eastward (Figures 4 and 5). It is also interesting to note that the region of maximum pressure falls between 0300 and 0900 GMT 19 February is located along the Virginia coast directly between the two distinct cloud

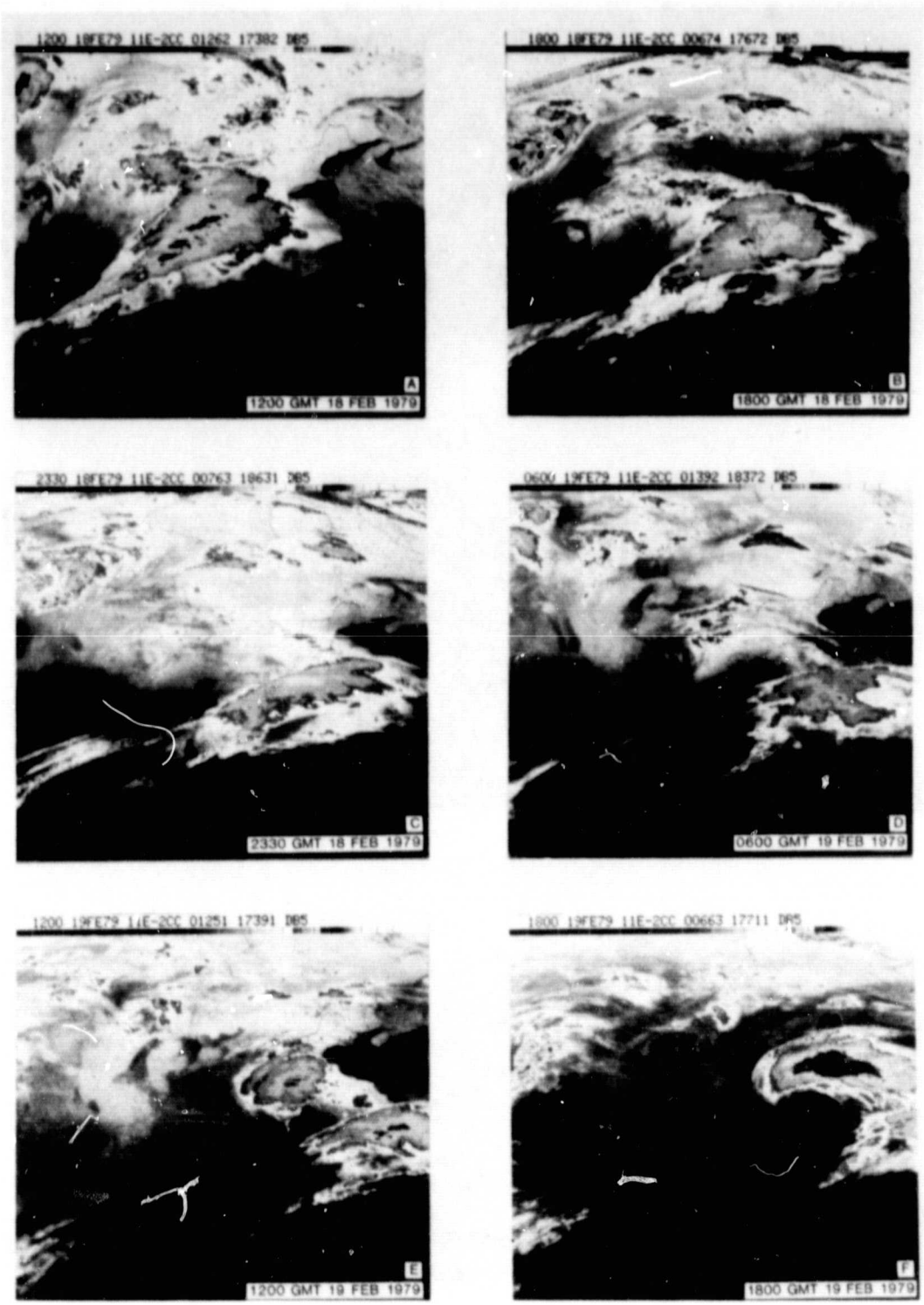

Figure 6. Six-hourly infrared satellite imagery prior to and during cyclogenesis. (A) 1200 GMT 18 February 1979. (B) 1800 GMT 18 February 1979. (C) 2330 GMT 18 February 1979. (D) 0600 GMT 19 February 1979. (E) 1200 GMT 19 February 1979. (F) 1800 GMT 19 February 1979.

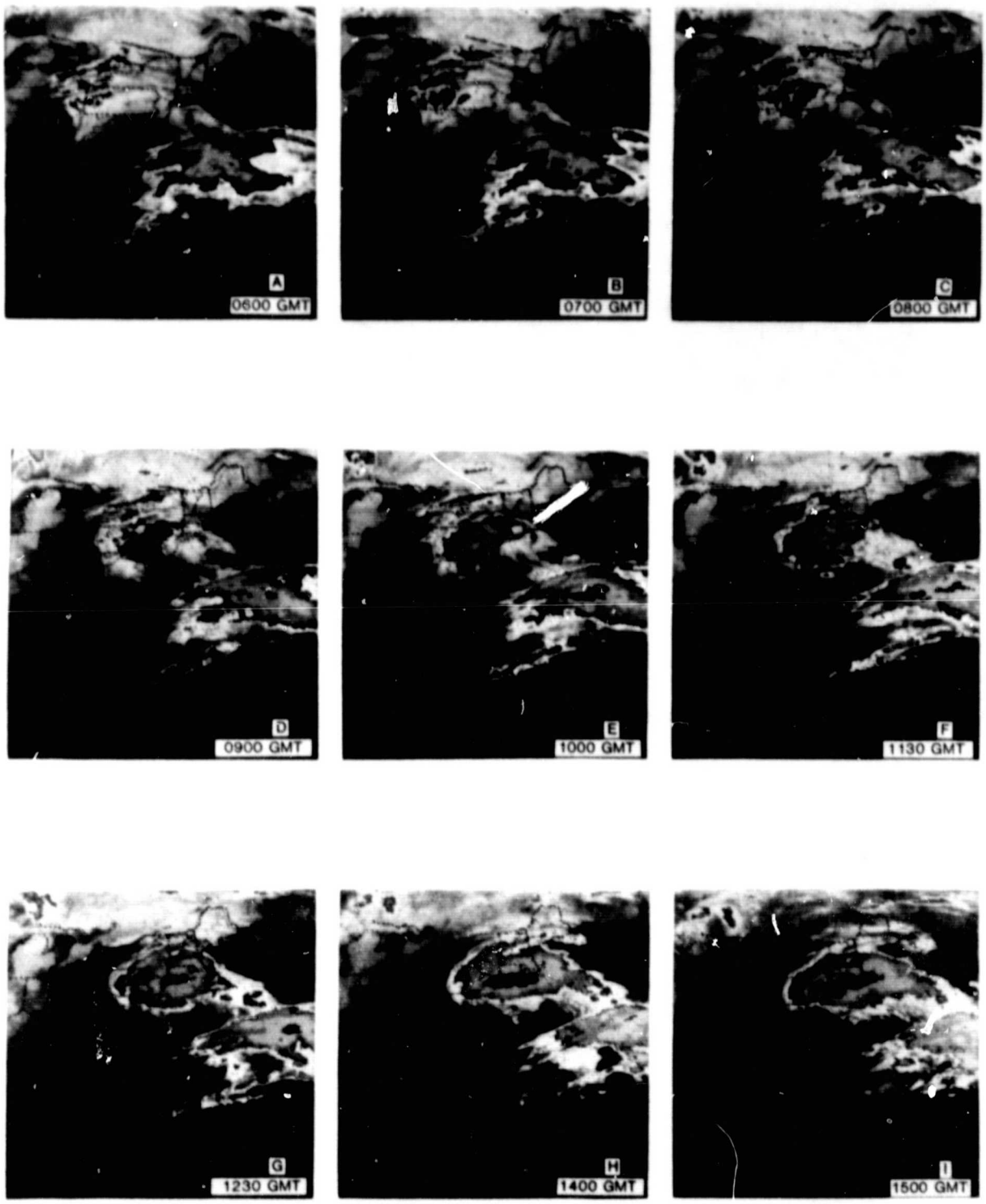

Figure 7. Infrared satellite imagery during cyclogenesis on 19 February 1979. (A) 0600 GMT. (B) 0700 GMT. (C) 0800 GMT. (D) 0900 GMT. (E) 1000 GMT. (F) 1130 GMT. (G) 1230 GMT. (H) 1400 GMT. (I) 1500 GMT.

masses, in an area where deep clouds were not observed (Figures 7A–7D). The banded structure of the lower level clouds over Virginia and the Del-Marva Peninsula (Figure 6D; Figures 7A–7C) illustrates the enhanced westward moisture flux from the Atlantic Ocean toward the expanding cloud mass to the north of the rapidly developing cyclone center.

The infrared imagery also illustrates the intense and rapid vortex development between 1200 and 1800 GMT 19 February (Figure 6F) as the cyclone rapidly deepened and moved east. It was during this period that convective cells developed immediately to the south of the vortex center (Figures 7F and 7G) and the cyclone and general cloud mass became more nearly colocated. It therefore appears that the influence of diabatic heating in the total evolution of the cyclone, particularly in the rapid vortex development, was maximized after 1200 GMT 19 February, approximately 9 hours after cyclogenesis commenced.

The infrared imagery lends evidence to the interpretation that cyclogenesis along the Carolina–Virginia coast was linked to the second Midwest wave propagating rapidly eastward. The area of intense snowfall did not move up the coast, but developed within the middle Atlantic region as the tropospheric wave propagated from the Ohio Valley. These observations suggest that the cyclone developed along the North Carolina–Virginia coast (probably within the northern extent of the inverted trough that developed during the 18th of February in conjunction with the coastal front) as the Ohio Valley wave encountered a region of lower static stability that was more conducive to cyclogenesis. This view is in contrast to the interpretation of a storm center simply moving north–northeast from the South Carolina–Georgia coast independent of the Ohio Valley wave. Resolving this aspect of the storm's development and propagation is crucial for future model and quasi-Lagrangian budget studies which depend, in part, on having a well defined storm track.

3. INTERACTION BETWEEN UPPER AND LOWER LEVEL JET STREAKS PRIOR TO CYCLOGENESIS AS ANALYZED WITHIN THE ISENTROPIC FRAMEWORK

In the previous section, several significant and dramatic changes in both upper and lower level wind fields were noted which appear to play a significant role in the development of the President's Day storm. The rapid development of the 850mb lower level winds along the southeastern coast between 0000 GMT and 1200 GMT 18 February (1) coincided with the amplification of the 300mb winds, (2) coincided with the intensification of snowfall rates in northern Georgia, Tennessee and the Carolinas, and (3) preceded the formation of the coastal front described by Bosart (1980). The development of the low level jet (LLJ), its relationship to the observed upper tropospheric accelerations and lower tropospheric mass distributions, and its interaction with the second tropospheric wave are described in this section.

Isentropic Analysis of the President's Day Cyclone

A detailed analysis of the interaction between the several jet streaks that influenced the cyclone's development is presented in this section through use of isentropic analyses on the 292, 312 and 332K surfaces and vertical cross section analyses.

The 292K surface is representative of the lower troposphere over the Southeast in which the strong LLJ developed by 1200 GMT 18 February. The 312K surface is representative of the middle troposphere over the central Midwest where the second tropospheric wave amplified by 0000 GMT 19 February. The 332K surface nearly parallels the tropopause, especially over the Southeast and provides a means for examining the maximum winds associated with the subtropical jet (STJ), which amplified between 0000 GMT and 1200 GMT 18 February.

The isentropic analyses presented in this report are subjective, but have been cross-checked with numerous cross sections and the NWS pressure analyses. The "cross-check" analysis procedure not only incorporates the detailed vertical resolution of individual rawinsonde ascents into the isentropic wind, pressure, and moisture analyses (Shapiro, 1970), but also insures horizontal and vertical consistency in the mass and wind fields among all the analyses.

The 332K, 312K and 292K analyses for 1200 GMT 17 February through 1200 GMT 19 February (Figures 8 to 12) reflect the same basic sequence as the pressure analyses described in Section 2. However, as discussed by Uccellini (1976), Uccellini and Johnson (1979) and Carlson (1980), the isentropic analyses provide a three dimensional perspective of interactive upper, middle and lower tropospheric flow regimes, especially with regard to moisture transports and coupled jet phenomena. The important points gleaned from the isentropic analyses are listed as follows:

1. The amplification of the subtropical jet between 1200 GMT 17 February and 1200 GMT 18 February, is depicted on the 332K surface (Figures 8, 9, and 10). During this period, the maximum winds along the axis of the STJ increased from 65 ms^{-1} to over 80 ms^{-1}. The maximum winds were located within the lowest pressure (highest altitude) on the 332K surface, indicating that parcels entering the STJ accelerated and rose to the level of maximum winds. A polar front jet (PFJ), depicted as a separate entity off the Delaware-New Jersey coast on the 332K surface in Figure 10, is directed toward higher pressure (lower altitude) implying that air was sinking as it entered the jet core. The distribution of clouds over the eastern United States is evidently related to the juxtaposition of these two different upper level jet streaks as analyzed within the isentropic framework. The western edge of the high cloudiness seen in the infrared satellite imagery (Figure 6A) aligns with the lower extension of the rising STJ (evident on the 312K surface in Figure 10) while concurrently the lack of clouds over the Northeast is associated with the confluence of two different air streams and the sinking PFJ.

2. The development of a low level jet in the Southeast on the 292K surface between 0000 GMT and 1200 GMT 18 February is marked by an increase of the winds from 5 ms^{-1} to over 25 ms^{-1} (Figures 9 and 10). The LLJ extended up from 900 mb to 750 mb in the Southeast (see Figure 10C) and was obviously transporting moisture into a region of moderate snow (Figure 3C). The subsequent evolution of the LLJ is illustrated in Figures 11 and 12 which show the LLJ propagating slowly up the East Coast, directed up toward the 750mb level, and

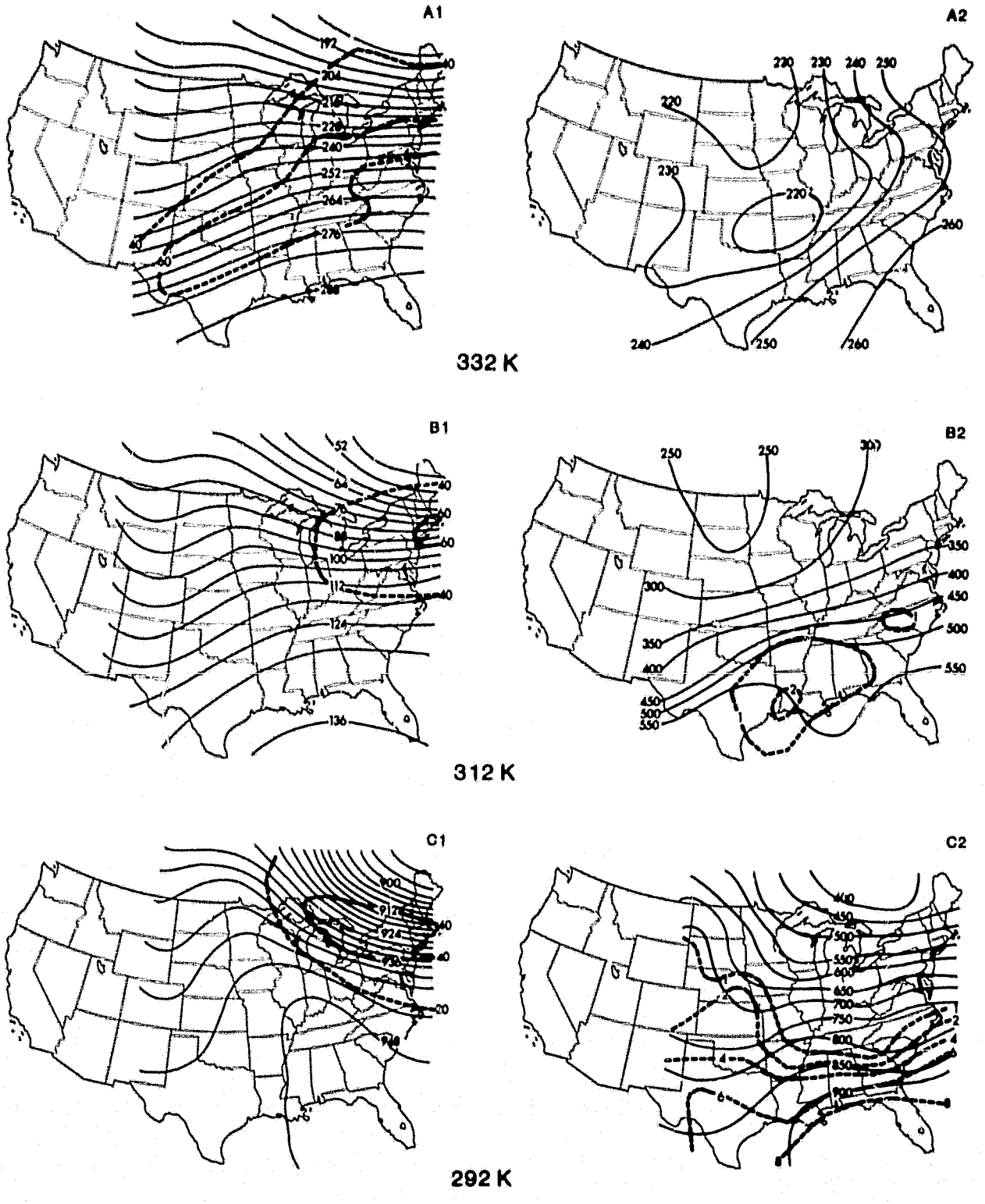

Figure 8. Isentropic analyses for 1200 GMT 17 February 1979. (A1) (B1) (C1): Montgomery Stream Function (Ψ) analysis, (solid, 240 = $3.240 * 10^5 m^2 s^{-2}$; 936 = $2.936 * 10^5 m^2 s^{-2}$) and isotach (dashed ms^{-1}) for 332°K, 312°K, and 292°K surfaces, respectively. (A2) (B2) (C2) Pressure (solid, millibars) and mixing ratio (dashed gkg^{-1}), for corresponding surfaces.

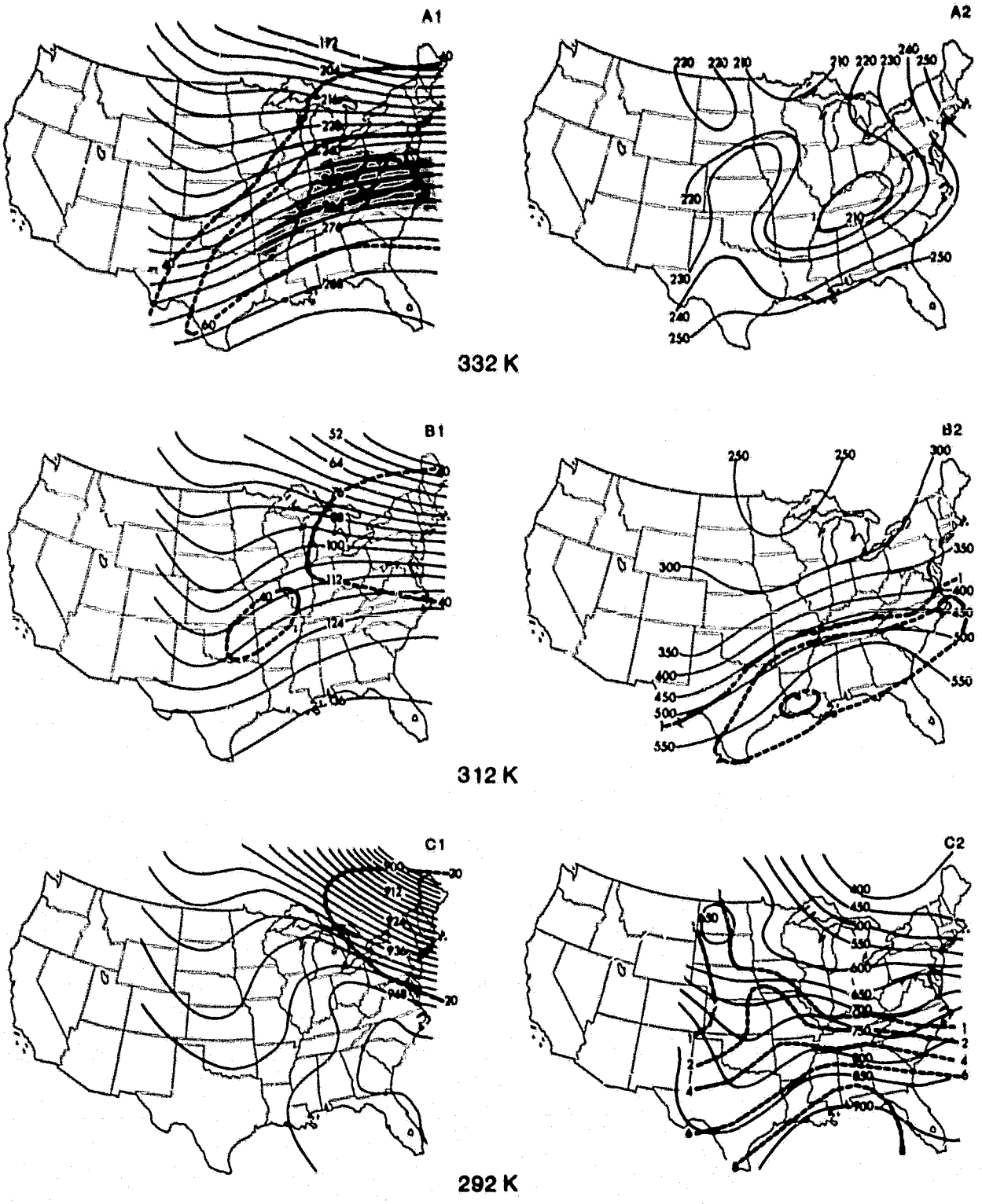

Figure 9. Isentropic analyses for 0000 GMT 18 February 1979. (A1) Shading represents velocities between 70 ms^{-1} and 80 ms^{-1}. See Figure 8 caption for additional details.

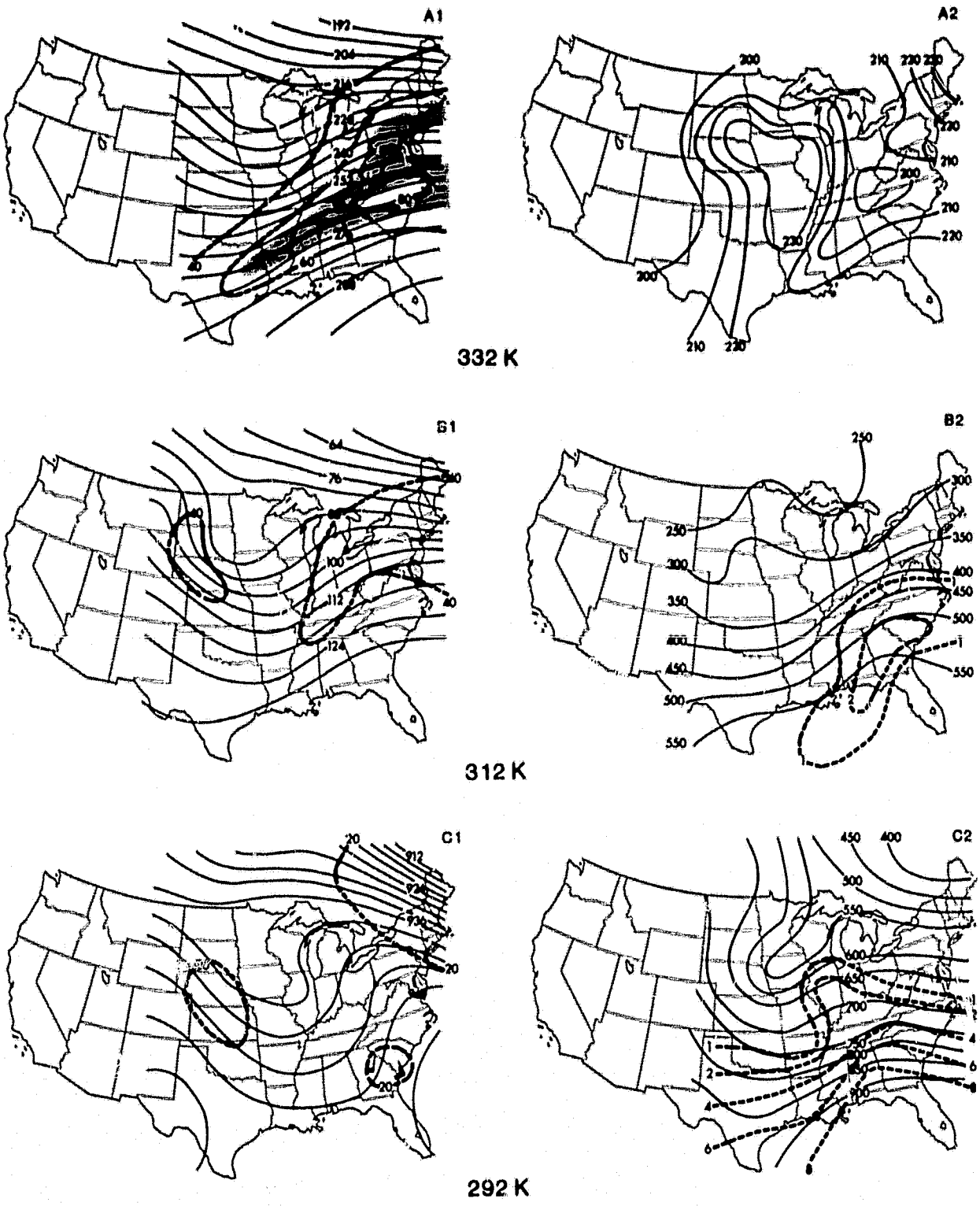

Figure 10. Isentropic analyses for 1200 GMT 18 February 1979. (A1) Shading represents velocities between 70 ms^{-1} and 80 ms^{-1}. (C1) Wind barbs represent largest measured velocities (each barb denotes a 10 ms^{-1} velocity; a half barb denotes a 5 ms^{-1} velocity). See Figure 8 caption for additional details.

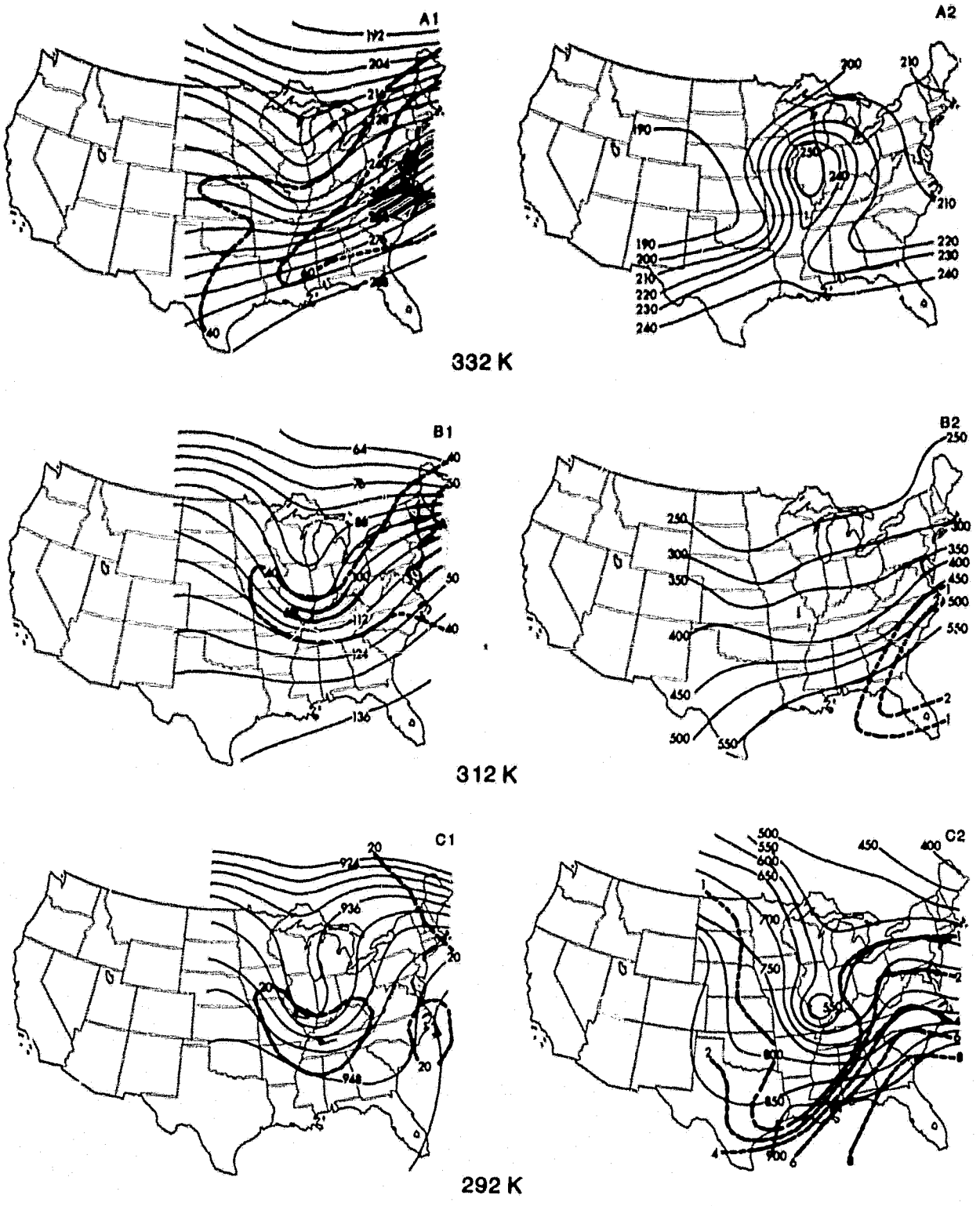

Figure 11. Isentropic analyses for 0000 GMT 19 February 1979. (A1) Shading represents velocities between 70 ms^{-1} and 80 ms^{-1}. (B1) Shading represents velocities between 50 ms^{-1} and 60 ms^{-1}. (C1) Wind barbs represent largest measured velocities. See Figure 8 caption for additional details.

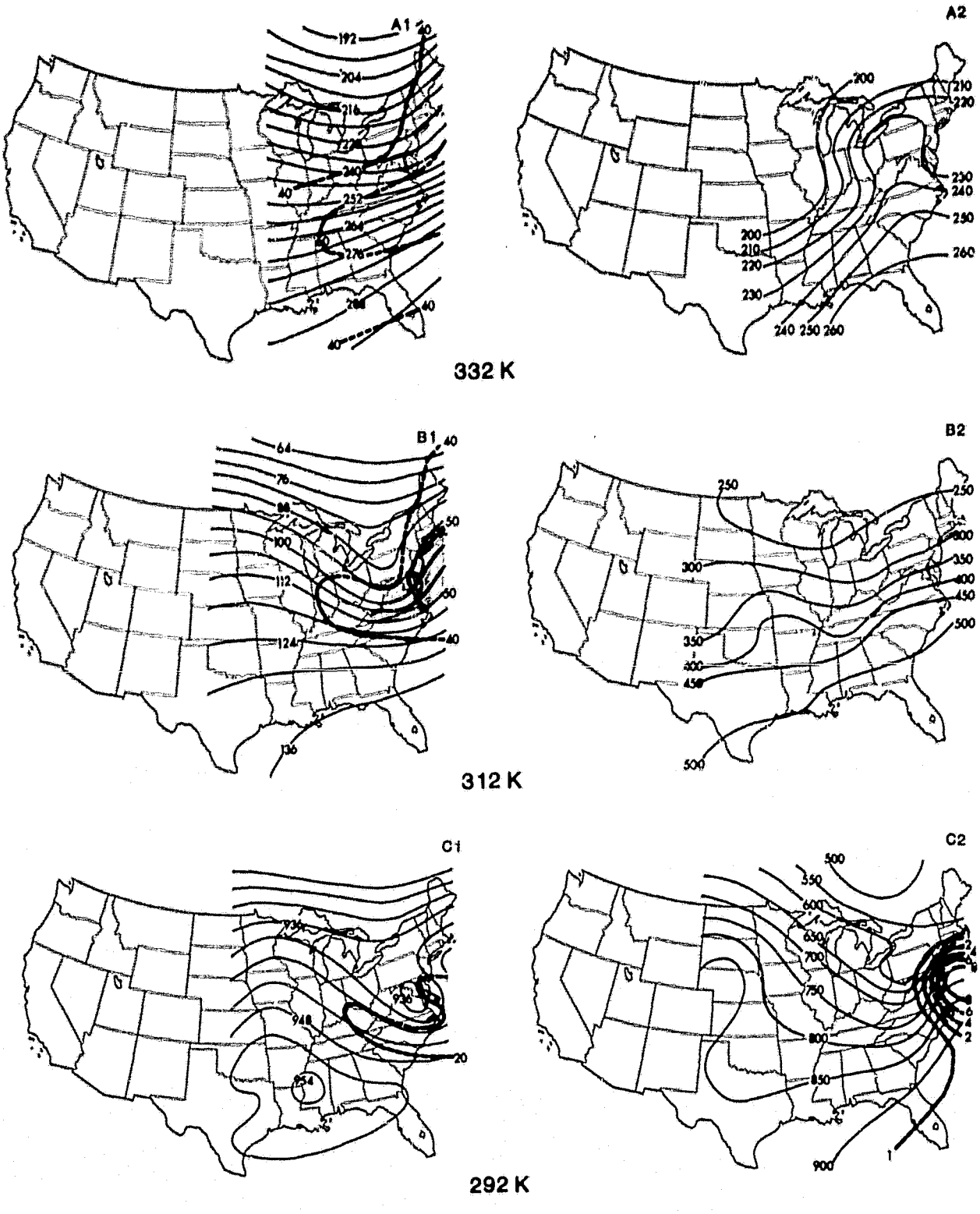

Figure 12. Isentropic analyses for 1200 GMT 19 February 1979. (B1) Shading represents velocities between 50ms^{-1} and 60ms^{-1}. (C1) Wind barbs represent largest measured velocities. See Figure 8 caption for additional details.

transporting moisture into regions of moderate and heavy snow. It is clear that the LLJ analyzed for this case is not solely a boundary layer phenomenon but extends well beyond the planetary boundary layer (PBL) towards the 700mb level.

3. The evolution of the "second wave," particularly its amplification over the Ohio Valley by 0000 GMT 19 February and propagation towards the East Coast by 1200 GMT 19 February is clearly illustrated on the 312K surface. Associated with the wave was a polar jet streak whose velocities were maximized between 300 and 400mb and increased in magnitude to greater than 50ms^{-1} by 0000 GMT 19 February (Figure 11). The lower extension of this jet is evident on the 292K surface, especially after 1200 GMT 18 February (Figures 10 to 12). The 292K wind maximum is characterized by a westerly flow nearly parallel to the Montgomery Stream Function (Ψ) contours and the 650 and 750mb isobars. Therefore, the nature of the lower extension of the polar jet is significantly different from the more ageostrophic LLJ which developed along the Southeast coast, accelerated toward lower Ψ values and ascended the 292K surface. The propagation of the middle tropospheric polar jet streak toward the East Coast and its apparent interaction with the low level jet moving up the coast (Figures 11 and 12) appear to be important factors in the cyclogenesis that commenced between 0000 GMT and 1200 GMT 19 February. It is interesting to note that the LLJ developed near the axis of the STJ (a relationship which is further explored in the following section) but eventually propagated into an exit region of a polar jet and was totally incorporated within the cyclone's circulation by 1200 GMT 19 February. This analysis reveals the complexities involved in describing the total evolution of the LLJ and its relationship to different jet systems during a cyclogenetic period in contrast to a more simplified interaction described by Uccellini and Johnson (1979) for a non-cyclogenetic period.

The vertical cross sections from Flint, Michigan (FNT) to Charleston, South Carolina (CHS) (Figure 13) illustrate the polar jets that affected the East Coast immediately prior to cyclogenesis. At 1200 GMT 18 February (Figure 13A) the LLJ located over CHS is maximized above the PBL near the 700mb level. The STJ is maximized near the 200mb level while the first polar jet (PJ1)

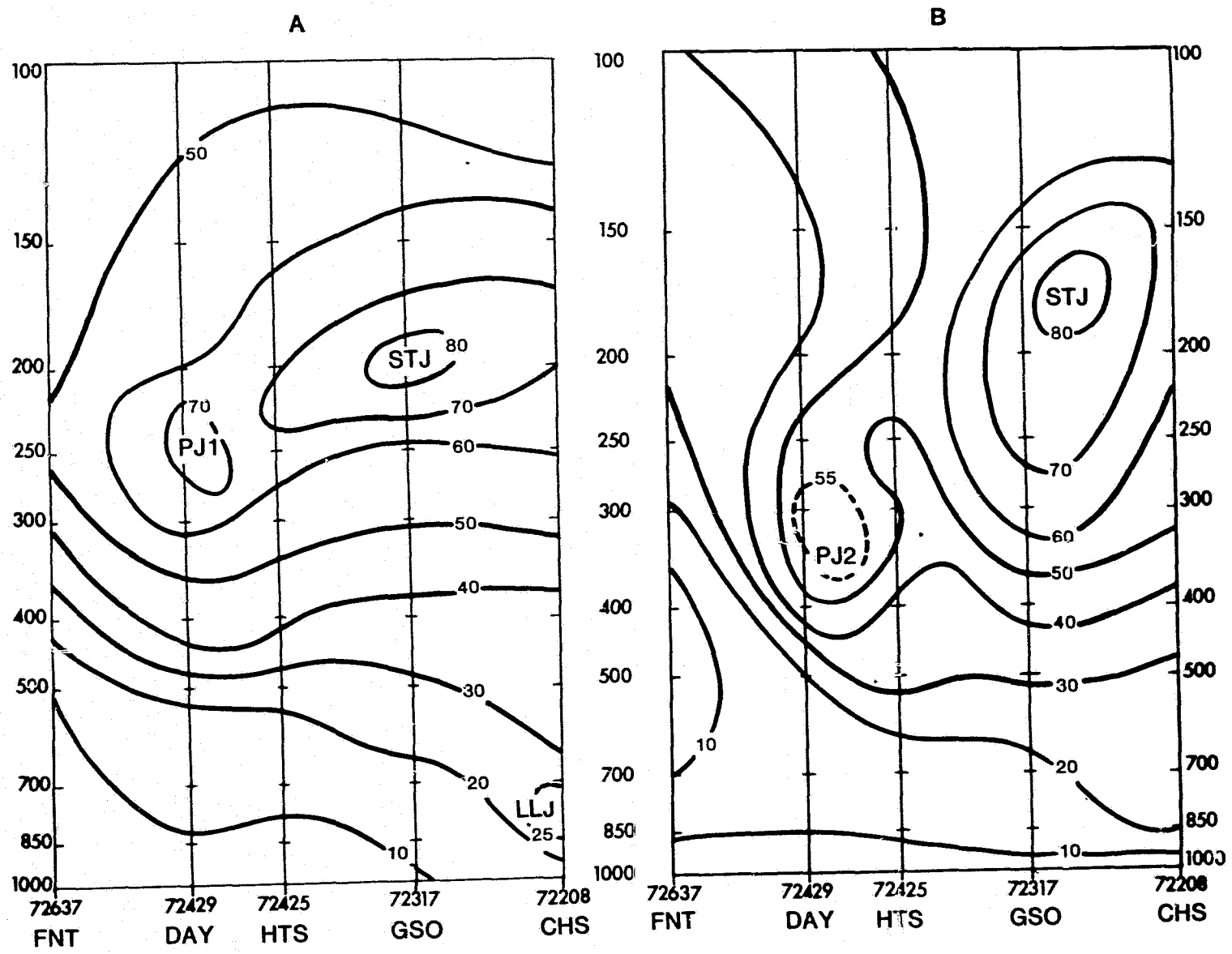

Figure 13. Vertical cross-sectional wind components (ms^{-1}) from Flint, Michigan (FNT) to Charleston, SC (CHS) for (A) 1200 GMT 18 February 1979; (B) 0000 GMT 19 February 1979. Abbreviations represent the following: STJ (subtropical jet), LLJ (low level jet), PJ1 (polar front jet associated with Northeast cold outbreak), PJ2 (polar front jet associated with Midwest wave).

that extended from the Ohio Valley to off the East Coast is maximized near 250mb. The polar jet associated with the second wave in the northern Midwest (PJ2) appears maximized near 350mb just south of Dayton, Ohio at 0000 GMT 19 February (Figure 13B).

Acceleration of the Subtropical Jet and Associated Mass Adjustments

As noted in the previous section, the STJ analyzed on the 332K surfaces accelerated from 65 to over 80ms^{-1} between 1200 GMT 17 February and 1200 GMT 18 February, immediately prior to and during the period of LLJ development. Figure 14 illustrates that during the period in which the STJ amplified, winds became noticeably supergeostrophic near the jet core at 0000 GMT 18 February (Figure 14B), and along the entire length of the STJ at 1200 GMT 18 February (Figure 14C).[1] The winds did not become subgeostrophic in the entrance region of this intense STJ until 0000 GMT 19 February (Figure 14D). Thus, geostrophic velocities did not increase to 80ms^{-1} over the Southeast (Tennessee Valley, see Figure 14D) until 24 hours after the accelerations in the STJ were first observed and 12 hours after the actual winds had increased to a magnitude greater than 80ms^{-1}.

Since the increase in the magnitude of the geostrophic winds significantly lagged the observed accelerations of the actual winds, it appears that the winds in the Southeast were not adjusting to the given local mass distribution. Rather, the accelerating supergeostrophic winds forced the mass to adjust in a manner similar to the adjustment concepts first described by Rossby (1938) for an infinitely long current (Figure 15). Rossby's theory shows that an unbalanced, supergeostrophic current will transport mass to the right (looking downstream) to bring the current into a geostrophically balanced steady state. Cahn's (1945) application of Rossby's theory illustrates that the adjustment of the mass field will "overshoot" the balanced state before

[1]The difference between actual and computed geostrophic velocities computed on the 332K surface in Figure 14 is consistent with the same differences computed for the National Weather Service 200-mb analyses. For the most part, gradient winds computed on the 332K surface were equivalent to the geostrophic values, given the large radius of curvature of the observed flow.

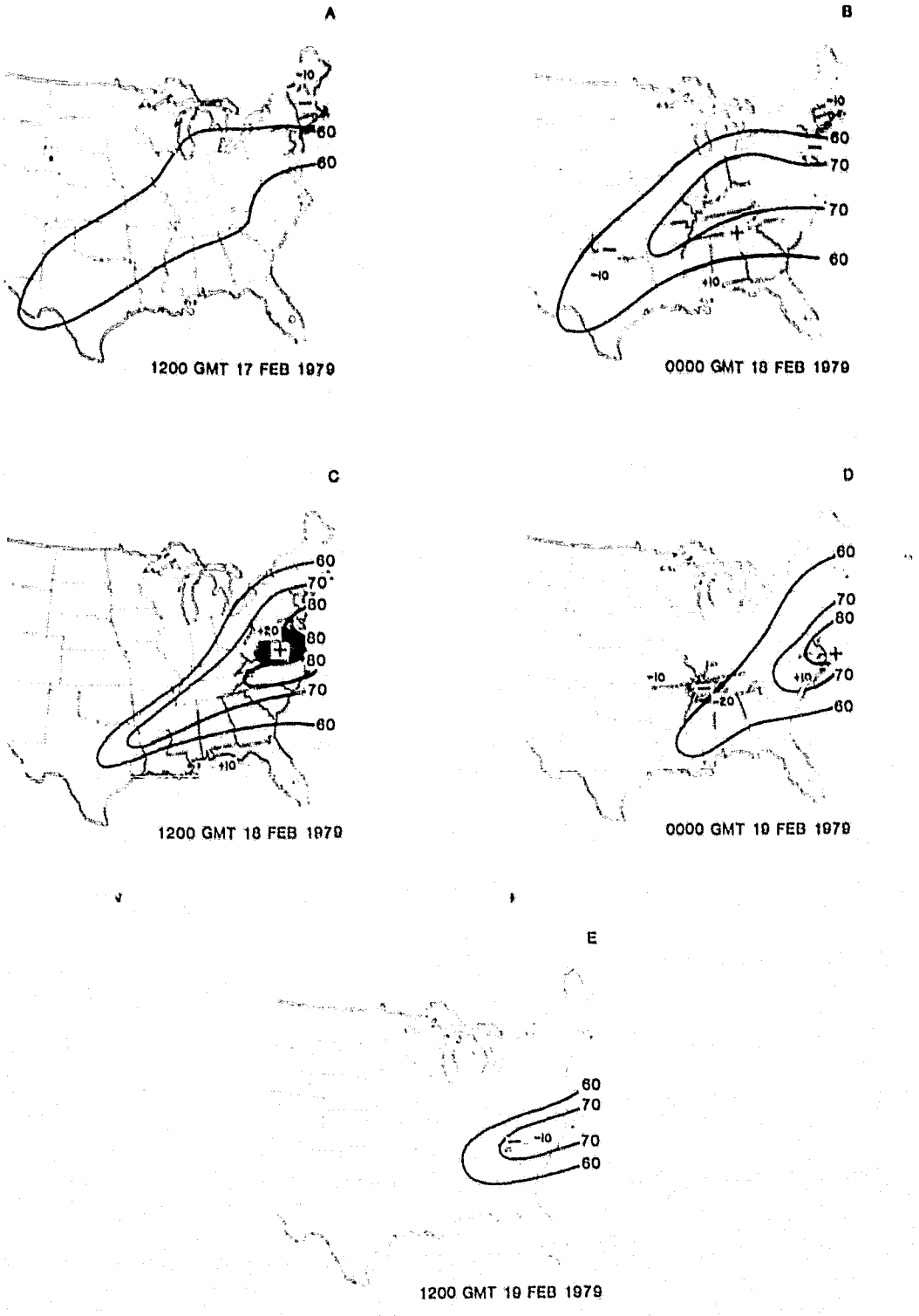

Figure 14. Evolution of the ageostrophic nature of the 332°K winds from 1200 GMT 17 February 1979 to 1200 GMT 19 February 1979. Contours indicate actual wind velocities (ms^{-1}). Shading represents whether winds are subgeostrophic (–) or supergeostrophic (+) by at least $10ms^{-1}$ or $20ms^{-1}$ (heavy shading).

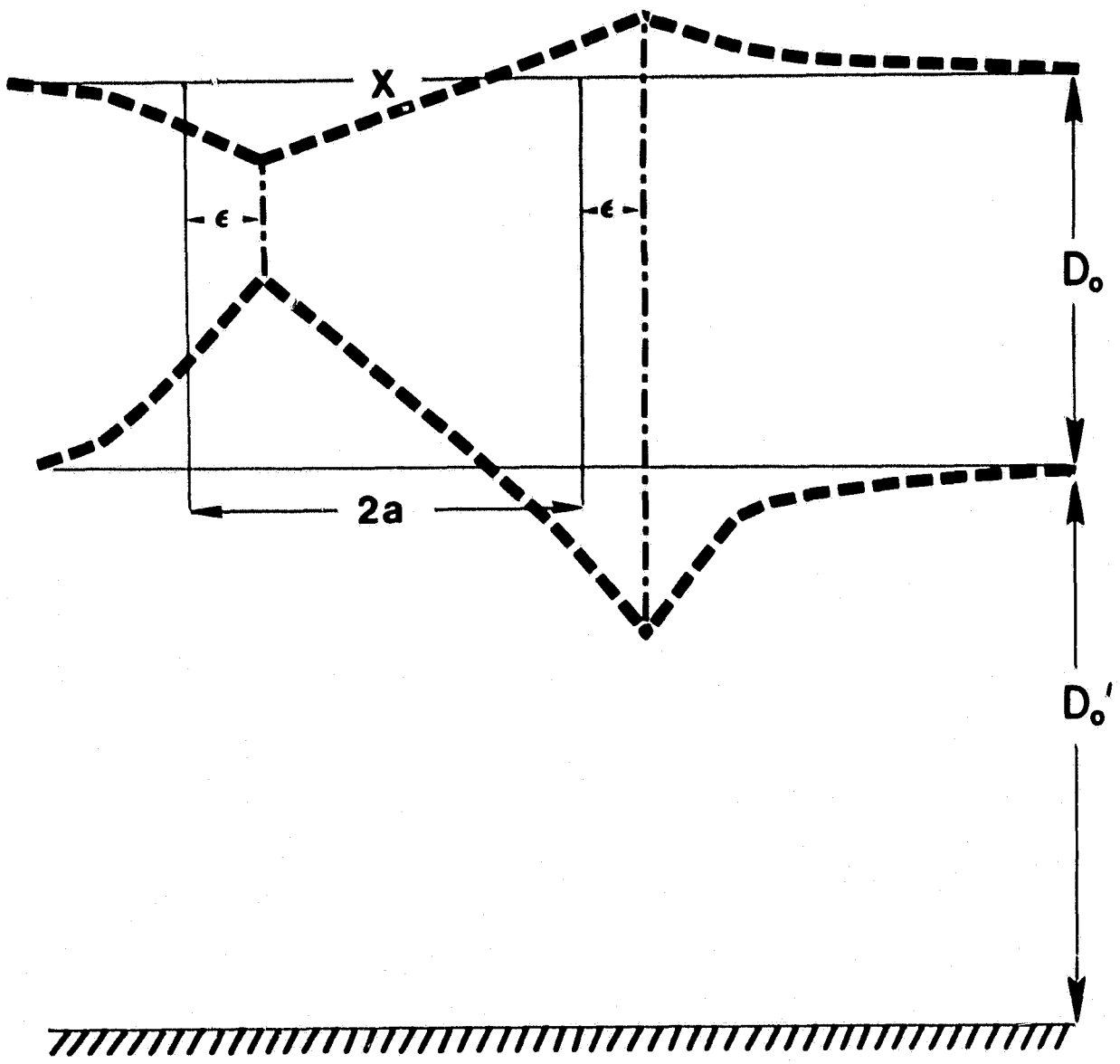

Figure 15. Schematic representation of a mass adjustment in a two layer infinite current (directed into the page). Within the top layer D_0, the development of supergeostrophic current of width 2a will lead to the righthand displacement (ϵ) of the current and the resultant mass redistribution (heavy dashed line). After Rossby (1938).

actually approaching the steady state solution and yield a slowly oscillating inertia-gravity wave. The finite length of the STJ described in this study as well as its accelerating nature complicate simple adjustment concepts. However, since the STJ over the Southeast appears to be supergeostrophic along the entire length for nearly 24 hours, a mass adjustment that would normally be found only within an indirect transverse circulation in the exit region of a finite length jet streak (Uccellini and Johnson, 1979, among others) should have occurred in this case along the entire length of the STJ between 1200 GMT 17 February to 0000 GMT 19 February.

The vertical isentropic cross sections from Peoria, Illinois (PIA) to Waycross, Georgia (AYS) (Figure 16) provide evidence for the cross stream mass adjustments forced by the supergeostrophic flow at the STJ level (Figures 14B and 14C). Between 1200 GMT 17 February and 0000 GMT 19 February, there is a persistent depletion of mass on the cyclonic side of the jet streak (J), as illustrated by the selected isentropes in Figure 16, within which the vertical pressure differential ($\partial p/\partial \theta$) decreases.[1] To the right of the STJ, $|\partial p/\partial \theta|$ consistently increases, indicating a net mass transport into that region. The rightward shift of the jet core during the period of most noticeable adjustment (Figure 16B to 16D) is also consistent with Rossby's theory, which predicts a rightward displacement (ϵ in Figure 15) of the current as the adjustment proceeds to a geostrophically balanced state.

The rapid amplification of the northwest to southeast tilted trough along the line of the cross section in Figure 16, evident on the 850mb (Figures 2B and 3B) and the 292K surfaces (Figures 9C1 and 10C1), is another indication of the importance of the cross stream mass adjustments in this case. The 332K pressure analyses in Figure 8A2 to 10A2 offer additional evidence. The consistent decrease of minimum pressure along or just to the right of the jet axis on

[1]Mass is defined within the isentropic framework by the volume integral $\int_V |1/g\ \partial p/\partial \theta|\, dV$. From Equation 4, page 13, mass convergence (divergence) will spread apart (bring together) isentropic surfaces and destabilize (stabilize) the atmosphere. See Uccellini (1976) for additional details.

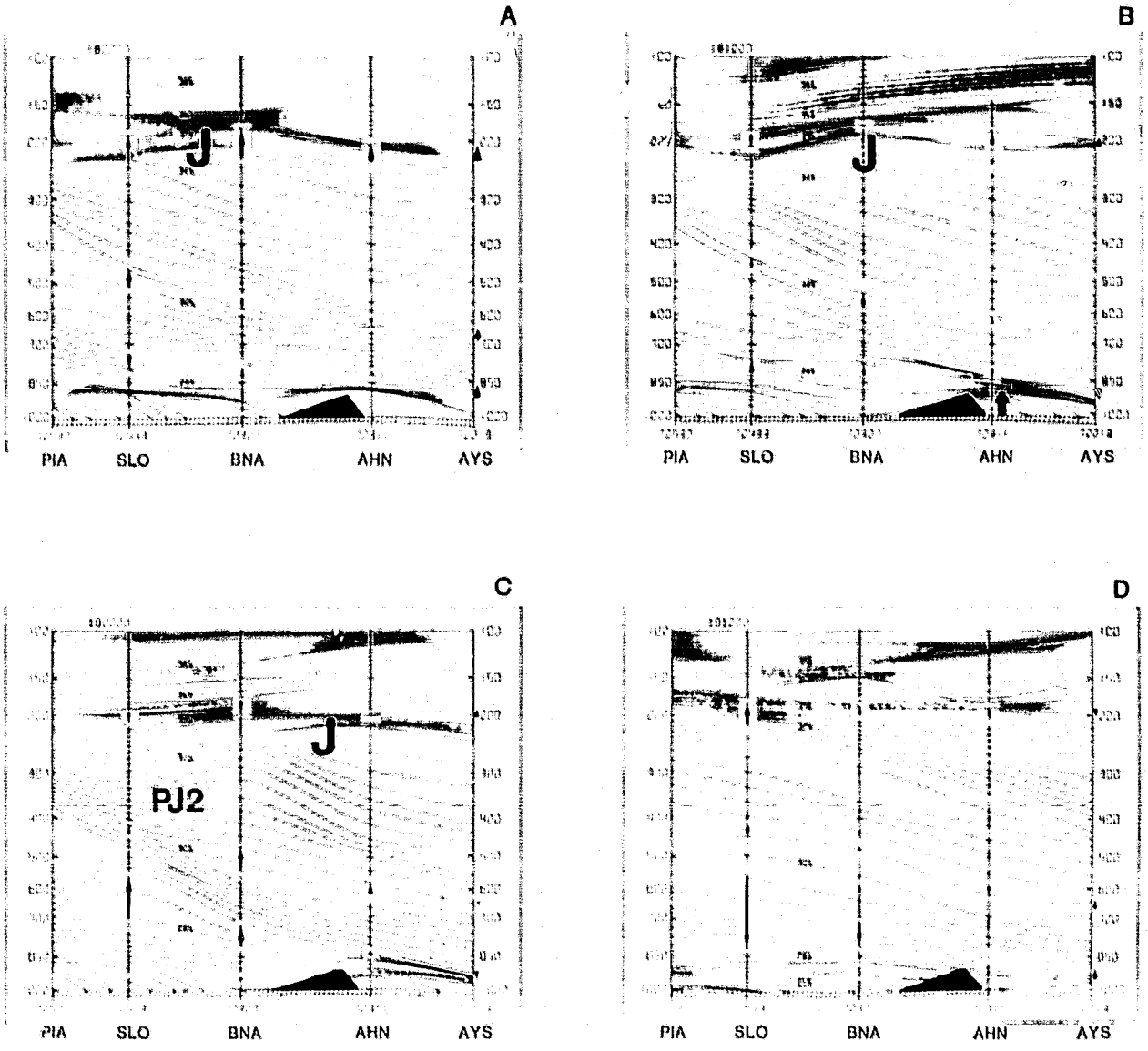

Figure 16. Vertical cross sections of potential temperature from 1200 GMT 17 February 1979 (top left) to 1200 GMT 19 February 1979 (bottom right). Arrows reflect movement of isentropic surfaces from previous time (end of arrow) to current position (head of arrow). J indicates location of the subtropical jet. (C) PJ2 indicates location of polar front jet associated with the Midwest wave.

the 332K surface illustrates that the upward "bulge" that normally marks the upper isentropic surfaces to the right of the jet core (see Figure 16) is amplifying in response to the increased mass transport into that region. It therefore appears that a cross-stream component of the mass transport related to an indirect transverse circulation forced by the supergeostrophic current is significant in this case and that the changes depicted in the cross sections (Figure 16) are not merely due to along-stream advections into the plane of the cross section.

Remaining questions concerning reasons for the observed accelerations of the STJ are addressed in Section 5.

Coupling the Mass Adjustments to an Isallobaric Forcing of the Low Level Jet

The "coupled" jet streak concept presented by Uccellini and Johnson (1979) relates the mass adjustments within the exit region of an upper level jet streak to the development of an LLJ through an isallobaric response to the mass adjustments. The coupling concept is applied to this case due to the ageostrophic nature, vertical extent and rapid development of the LLJ and its close proximity to an upper tropospheric jet streak.

The basic equations used for the analysis of coupled jet streaks involves approximating the ageostrophic wind component ($\underset{\sim}{U}_{ag}$) by

$$\underset{\sim}{U}_{ag} = f^{-1}\left[\underset{\sim}{k} \times \frac{\partial \underset{\sim}{U}_g}{\partial t_\theta} + \underset{\sim}{U} \cdot \underset{\sim}{\nabla}_\theta \left(\underset{\sim}{k} \times \underset{\sim}{U}_g\right)\right], \qquad (1)$$

where: term (1) represents the isallobaric wind and (2) represents the inertial advective wind, using a geostrophic momentum approximation, f is the Coriolis term, $\underset{\sim}{k}$ is the unit normal vertical vector, $\underset{\sim}{U}_g$ is the geostrophic wind, $\underset{\sim}{U}$ is the actual wind and the subscript θ refers to the terms being computed on isentropic surfaces. The isallobaric wind ($\underset{\sim}{U}_{ag_i}$) reduces to

$$\underset{\sim}{U}_{ag_i} = -f^{-2}\left(\underset{\sim}{\nabla}_\theta \frac{\partial \Psi}{\partial t}\right) \qquad (2)$$

where Ψ is the Montgomery Stream Function. As derived by Uccellini and Johnson, $\underset{\sim}{U}_{ag_i}$ can be defined on any arbitrary isentropic surface (θ_L) by

$$\underset{\sim}{U}_{ag_i}(\theta_L) = \frac{-R}{f^2}\left\{\underset{\sim}{\nabla}\left[\frac{T_s}{p_s}\frac{\partial p_s}{\partial t_\theta}\right] + \underset{\sim}{\nabla}\left[\int_{\theta_s}^{\theta_L}\left(\frac{p}{p_{oo}}\right)^{\kappa}\frac{1}{p}\frac{\partial p}{\partial t_\theta}\,d\theta\right]\right\} \tag{3}$$

where R is the Universal Gas Constant, T and p are temperature and pressure respectively, p_{oo} is a reference pressure and the subscript s refers to surface values. The form of (3) reveals that the isallobaric wind in isentropic coordinates is determined by the gradients of surface pressure tendency and the integrated pressure tendency between the earth's surface and Ψ_L. The relationship between the pressure tendencies and $\underset{\sim}{U}_{ag_i}$ expressed in (3) couples tropospheric mass adjustment to the isallobaric wind on θ_L. The vertical integration of the mass continuity equations between arbitrary lower and upper isentropic surfaces (θ_2 and θ_1) yields

$$\frac{\partial p_2}{\partial t} = \frac{\partial p_1}{\partial t} + \int_{\theta_2}^{\theta_1}\left[\underset{\sim}{\nabla}_\theta\cdot\frac{\partial p}{\partial \theta}\underset{\sim}{U} + \frac{\partial}{\partial \theta}\left(\frac{\partial p}{\partial \theta}\frac{d\theta}{dt}\right)\right]d\theta. \tag{4}$$

With the substitution of (4) into (3), the isallobaric ageostrophic component on θ_L can be linked to horizontal mass divergence and diabatic processes.

The Ψ tendencies and resultant isallobaric winds as defined by (2) are presented in Figure 17 for the 48-hour period preceding cyclogenesis. Between 0000 GMT and 1200 GMT 18 February an area of maximum Ψ falls on the 292K surface coincided with the STJ analyzed on the 332K surface and amplified to $-45 \times 10^1 m^2 s^{-2}$ as the area shifted southeastward. A second area of maximum Ψ falls was located in Ohio associated with the second wave propagating through the Ohio Valley (Figures 4 and 11). The existence of two centers of Ψ falls preceding cyclogenesis is consistent with other major cyclones as recently discussed by Weber (1980). By 1200 GMT 19 February a tremendous amplification of the Ψ falls had occurred along the Virginia coast, apparently reflecting either a phasing together of the two systems and/or an amplification of the $\partial\Psi/\partial t$ field propagating from Ohio toward the East Coast. The large amplitudes of both positive and negative centers of $\partial\Psi/\partial t$ are undoubtedly important features of the cyclogenesis

occurring along the coast and by (3) and (4) are indicative of the tremendous mass adjustments associated with the storm's development.

Figure 17 reveals that between 0000 GMT and 1200 GMT 18 February east to southeast isallobaric wind components approaching 5 ms^{-1} were found near and below the 850 mb level on the 292K surface, coinciding with the position of the LLJ observed at 1200 GMT 18 February (Figures 3B and 10C1). The development of the LLJ between 0000 and 1200 GMT 18 February occurred not only as the maximum $\partial\Psi/\partial t$ center continued to amplify and shift toward the southeast, but also as the center of maximum Ψ falls shifted toward higher pressure (lower altitude). It is also during this period that 850 mb height tendencies displayed a noted amplification. The same basic pattern persists at 0000 GMT and 1200 GMT 19 February as the area of maximum lower level winds is consistently found where the easterly isallobaric winds are maximized along the coast near the 850 mb isobar, just to the north and east of the maximum Ψ falls. It should be noted that the magnitudes of isallobaric winds along the coast are probably an underestimate since it was necessary to smooth the Ψ analysis due to the scarcity of data in that region, leading to a weakening of the gradients. The 12-hour time step also acts to reduce the magnitude of the isallobaric wind, especially during periods of rapid amplification.

An analysis of the inertial advective contributions to the ageostrophic wind (term 2 of Equation 1) reveals that the confluent nature of the flow upwind of the low level jet yielded an ageostrophic wind of 5 ms^{-1} at 1200 GMT 18 February. The isallobaric and inertial effects, thus, combine to produce a significant ageostrophic wind and subsequent parcel accelerations into the core of the LLJ in a manner similar to that described by Uccellini and Johnson (1979) and Uccellini (1980). An averaged value of 7.0 ms^{-1} for the ageostrophic component perpendicular to the direction of the LLJ over the 12-hour period (0000-1200 GMT 18 February) yields a 24 ms^{-1} increase in the wind along the axis of the observed LLJ, which compares favorably with observations (Figures 9 and 10).

An evaluation of (3) for the cross sections (Figure 16) between 0000 GMT and 1200 GMT 18 February with θ_L set equal to 290 K, directly links the mass changes depicted in the cross sections (Figure 16) to the 292 K isallobaric wind within the plane of the cross section or along the LLJ axis at 1200 GMT 18 February near Athens, Georgia (AHN). As is measured by the integrated pressure tendency term in (3), the increase (decrease) of pressure on the lower isentropic surfaces to the right (left) of the upper level jet will produce a lower tropospheric isallobaric wind directed toward the cyclonic side of the upper level jet (see Figure 7 in Uccellini and Johnson, 1979). In this case, the surface pressure tendency term contributed to a small isallobaric wind directed toward the coast, opposite to the direction of the LLJ. The integrated pressure tendency term contributed to an isallobaric wind of 2.7 ms^{-1} averaged over the area bounded by AYS and AHN and directed toward AHN. The contribution of the integrated pressure tendency term clearly accounts for the southeast isallobaric wind components analyzed in southern Georgia and along the coast in Figures 17B and 17C. Therefore, the lower tropospheric isentropes forced to higher pressure immediately along the coast and toward lower pressure beneath the jet core at 1200 GMT 18 February (Figure 16) increased the magnitude of the isallobaric wind in the vicinity of the rapidly developing LLJ. Thus, it appears that the mass adjustments associated with the supergeostrophic STJ played a significant role in the rapid acceleration of the low level winds in the Southeast. However, an added factor must be considered for the development of the LLJ in this case.

The "Damming Effect" of Cold Air on the Isallobaric Wind

The 10K decrease of the surface potential temperature at Athens, Georgia during the 12h period ending at 1200 GMT 18 February (as illustrated by the emergence of five isentropes into the PBL from below ground in Figure 16C) is a manifestation of the "damming effect" between the Appalachian Mountains and the East Coast (Richwein, 1980). The surface maps (Figures 1C–5C) and cross sections (Figure 16) both illustrate that the southward bulge in the surface anticyclone to the east of the Appalachian Mountains firmly establishes a shallow layer of very cold air

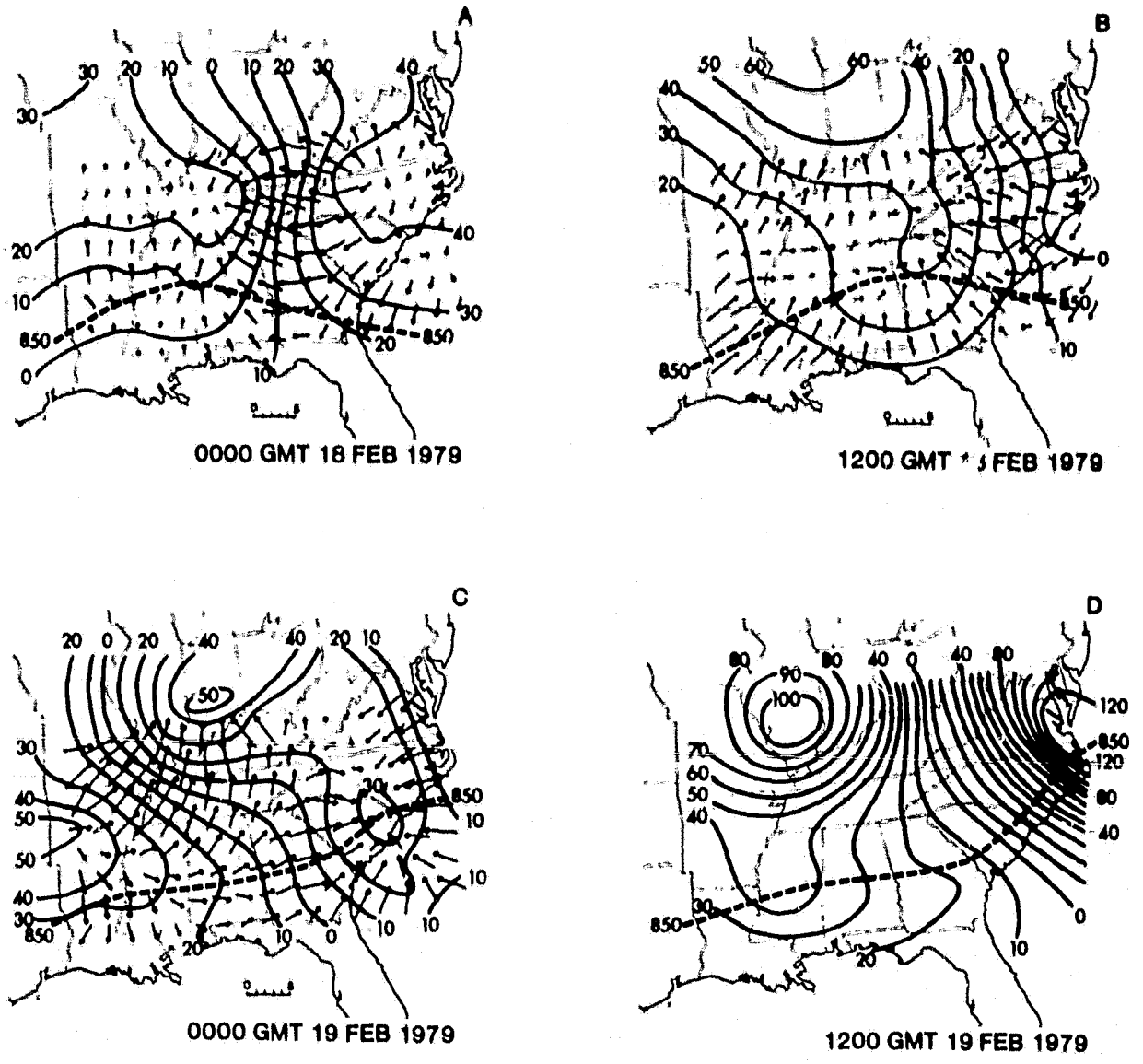

Figure 17. Evolution of the 12-hour tendency of Montgomery Stream Function (Ψ) and isallobaric winds on the 292°K surface from 1200 GMT 17 February 1979 to 1200 GMT 19 February 1979. Contours represent Ψ tendencies ($-40 = -40 * 10^1\ m^2 s^{-2}$). Vectors (A) (B) (C) [whose magnitudes (in ms^{-1}) are scaled immediately above each figure's time date] represent the isallobaric winds. The heavy dashed lines represent the 850mb contour.

southward to Georgia. Richwein used Schwerdferger's (1973) mountain barrier study to determine that when a shallow, stable cold air mass is forced against the eastern slopes of the Appalachians, a significant low level east-west pressure gradient is established, which in turn, continually reinforces the southward push of cold air between the Appalachian Mountains and the coast.

In this case, the persistent and self sustaining southward advection of colder air immediately east of the Blue Ridge Mountains modified the isallobaric response to the mass adjustments related to the STJ. The rapid emergence of the 272K to 263K isentropes into the boundary layer at AHN between 0000 GMT and 1200 GMT and the formation of a very stable layer near 850mb (Figures 16B and 16C) are not only indications of the damming effect but also contribute to a significant negative Ψ tendency for the lower level isentropic surfaces. The integrated pressure tendency at AHN, associated with the emerging isentropic surfaces (in Figure 16C) could account for the amplification of the negative Ψ tendency field from -20 to -40 x $10^1 m^2 s^{-2}$ (Figures 16A and 16B) between 0000 and 1200 GMT 18 February. The damming effect therefore localizes and amplifies the negative tendencies region and acts to enhance the gradients measured in (3) between the coast and the mountain range. The damming process could therefore act to increase the isallobaric wind directed toward the mountainous region along the cross section in Figure 17 and contribute to the development of the LLJ.

There is no attempt made here to rate the relative importance of the adjustments in the lower tropospheric momentum field forced by the supergeostrophic STJ and the damming of cold air east of the Appalachians. The importance of the STJ is illustrated by the fact that significant negative Ψ tendencies and resultant isallobaric flow existed west of the mountains at 0000 GMT 18 February as the STJ went noticeably supergeostrophic. The amplification of the Ψ tendency field at a higher pressure level on the 292K surface by 1200 GMT 18 February can be linked in part to the increase of the supergeostrophic component of the STJ and subsequent mass adjustment. The damming effect, which acts to focus the center of the negative Ψ tendencies just to the east of the Appalachians, could further amplify the Ψ tendency and increase the

gradients between the ocean and the mountains and, therefore, yield a larger isallobaric component. The lack of data off the coast prevents a strict comparison of these two processes, since the upper air analysis had to be smoothed, possibly yielding underestimates of all gradients along the coast.

Implications of the Isallobaric Forcing of the LLJ Upon the Pre-Cyclogenesis Snowfall

The development of the LLJ by 1200 GMT 18 February coincided with the development of the moderate to heavy snow in the Southeast (Figure 3C). As was the case in the Uccellini and Johnson (1979) study, the development of the LLJ directed up sloped isentropic surfaces significantly increased the moisture advection into the region of heaviest precipitation (seen by the combined wind, moisture and pressure analyses in Figures 10C1 and 10C2). The continued advection of moist air into the region of heaviest precipitation along the coast is maintained through 1200 GMT 19 February (Figures 11C and 12C). The convergent nature of the isallobaric wind also plays a significant role in enhancing the precipitation along the East Coast. The heaviest precipitation is persistently found near the region of maximum Ψ falls, such as the western Carolinas and eastern Tennessee at 1200 GMT 18 February, southern Virginia and southern Ohio at 0000 GMT 19 February and eastern Maryland at 1200 GMT 19 February (Figure 17). Evidently, the isallobaric wind plays a dual role in that its contribution to the forcing of the LLJ enhances the moisture transport into the precipitation area while the convergent nature of the wind aids in generating the precipitation.

The local circulation near the coastal front that developed after 1200 GMT 18 February could also act to enhance heavy precipitation, as discussed by Bosart (1975, 1977, 1980) and Marks and Austin (1979). It is interesting to note that the development of the highly ageostrophic LLJ and the damming of cold air just east of the Blue Ridge Mountains immediately preceded the onset of coastal frontogenesis. It is possible that the northerly ageostrophic wind over land (related to the damming effect) combined with the east-southeast lower tropospheric ageostrophic flow along the coast (forced by the jet streak related mass adjustments) could

provide the ageostrophic deformation field needed for coastal frontogenesis (Bosart, 1972) through shearing deformation.[1] Once coastal frontogenesis commences, a smaller scale circulation is forced along the front, which enhances precipitation rates, a process that was clearly evident at 0000 GMT 19 February along the North Carolina coast and 1200 GMT 19 February in the Washington, D.C. area (Bosart, 1980).

Scenario for the President's Day Cyclone

The following sequence of events is listed as a plausible scenario for the cyclogenesis period that marked the President's Day cyclone, February 17–19, 1979.

- Between 1200 GMT 17 February and 1200 GMT 18 February, an amplification of the STJ occurred yielding upper level winds that were at least 20 ms^{-1} supergeostrophic and forcing a mass transport from the cyclonic to the anticyclonic (northwest to southeast) side of the STJ.

- An LLJ formed in the Southeast by 1200 GMT 18 February in response to, in part, the mass adjustments forced by the supergeostrophic STJ. The "damming effect" (Richwein, 1980) on the east slopes of the Blue Ridge Mountains amplified the isallobaric wind response along the Southeast coast by significantly contributing to the negative Ψ tendencies maximized in northern Georgia.

- The development of the LLJ enhanced the precipitation rates from Georgia to Virginia by two processes. First, the development of the LLJ significantly increased the moisture transport into the region where the heavy snowfall occurred. Second, the enhanced convergence related to the isallobaric wind and the LLJ directed up the sloped isentropic surfaces increased and localized upward vertical motion. These two effects combined to yield the heavy snowfall associated with the first distinct area of precipitation as revealed by the SMS-GOES IR imagery.

[1] D. Keyser, personal communication.

- The development of the highly ageostrophic LLJ of the 18th of February and the damming of the cold air just east of the Blue Ridge Mountains immediately preceded and probably contributed to the onset of coastal frontogenesis through shearing deformation.

- The increased advections associated with the LLJ after 1200 GMT 18 February helped set up a lower tropospheric thermal ridge along the coast (as analyzed by Bosart, 1980), of which the coastal front is part, and thus primed the North Carolina-Virginia coast for cyclogenesis.

- An amplification of a second wave propagating into the Ohio Valley and its associated polar jet approached the East Coast by 0600 GMT 19 February and appeared to initiate the cyclogenesis near the northern portion of the thermal ridge. The SMS-GOES IR imagery indicates that the cloud mass associated with the cyclone rapidly developed and expanded in response to this rapidly propagating wave. The phasing of two separate Ψ tendency areas immediately prior to cyclogenesis is consistent with Weber's (1980) recent observations of major cyclogenesis.

- The heavy snow in the Washington, D.C. area and points north was due to the development and expansion of the second cloud mass associated with the intensifying cyclone after 0600 GMT 19 February. The precipitation rates were related, in part, to the accelerated moisture transport associated with the low level jet and the convergent nature of the isallobaric winds and were more locally enhanced by a pronounced coastal front, which extended north from this cyclone center (Bosart, 1980).

- The storm vortex rapidly developed and intensified, apparently aided by the low static stability over the oceans and by diabatic processes associated with sensible and latent heat release as discussed by Bosart (1980).

4. LFM-II MODEL SIMULATION

Bosart (1980) has discussed the failure of the NMC LFM-II to adequately forecast the rapid formation of the President's Day cyclone and heavy snowfall in the Middle Atlantic states. Bosart's analysis stresses the need for a better representation of the boundary layer (both in vertical resolution and physical parameterizations) and the use of significant level data in the lower

troposphere to better forecast the East Coast cyclogenesis. The purpose of this section is to study the LFM-II simulations of the upper and lower level jets to determine if these features were properly resolved within the model. The intent is not necessarily to make recommendations for model changes, but to determine the usefulness of LFM-II simulations for the study of jet streak dynamics which would otherwise suffer from the spatial and temporal aliasing inherent within the operational data base. Model output data initialized at three times prior to cyclogensis, [(1) 0000 GMT 18 February 1979, (2) 1200 GMT 18 February 1979, and (3) 0000 GMT 19 February 1979] are utilized for this study. The data used in this section have been post-processed in a manner described in the Appendix.

Description of the LFM-II Forecasts

The amplitude and propagation of the short wave that crossed the Ohio Valley and initiated the cyclone's rapid intensification along the East Coast were adequately forecast by the three LFM-II model runs initialized prior to 1200 GMT 19 February 1979 (Figure 18). A comparison between the actual 500mb geopotential at 1200 GMT 19 February 1979 and three forecasts of the same fields initialized 12, 24, and 36 hours prior to the verifying time (Figure 18) reveals that the 12- and 24-hour forecasts of the second wave were quite good while the 36-hour forecast underestimated the wave's amplitude. Figure 19 illustrates that ageostrophic transverse circulations in the entrance and exit regions of the polar jet associated with the Ohio Valley wave fit the conceptual model of jet streak circulations discussed by Bjerknes (1951), Riehl, et al. (1952), and Uccellini and Johnson (1979) among others. By 1200 GMT 19 February the merger between the polar jet and pre-existing subtropical jet had occurred in the model simulation. A significant transverse ageostrophic wind component directed from the cyclonic to anticyclonic side of the jet can be seen in the exit region immediately off the coast. The existence of a transverse ageostrophic wind component and strong vorticity advection (Figure 18) over the region where cyclogenesis actually occurred is consistent with the conceptual models of the influence of jet streaks upon cyclogenesis (Reiter, 1963) and quasi-geostrophic concepts (Bosart, 1980). An inspection

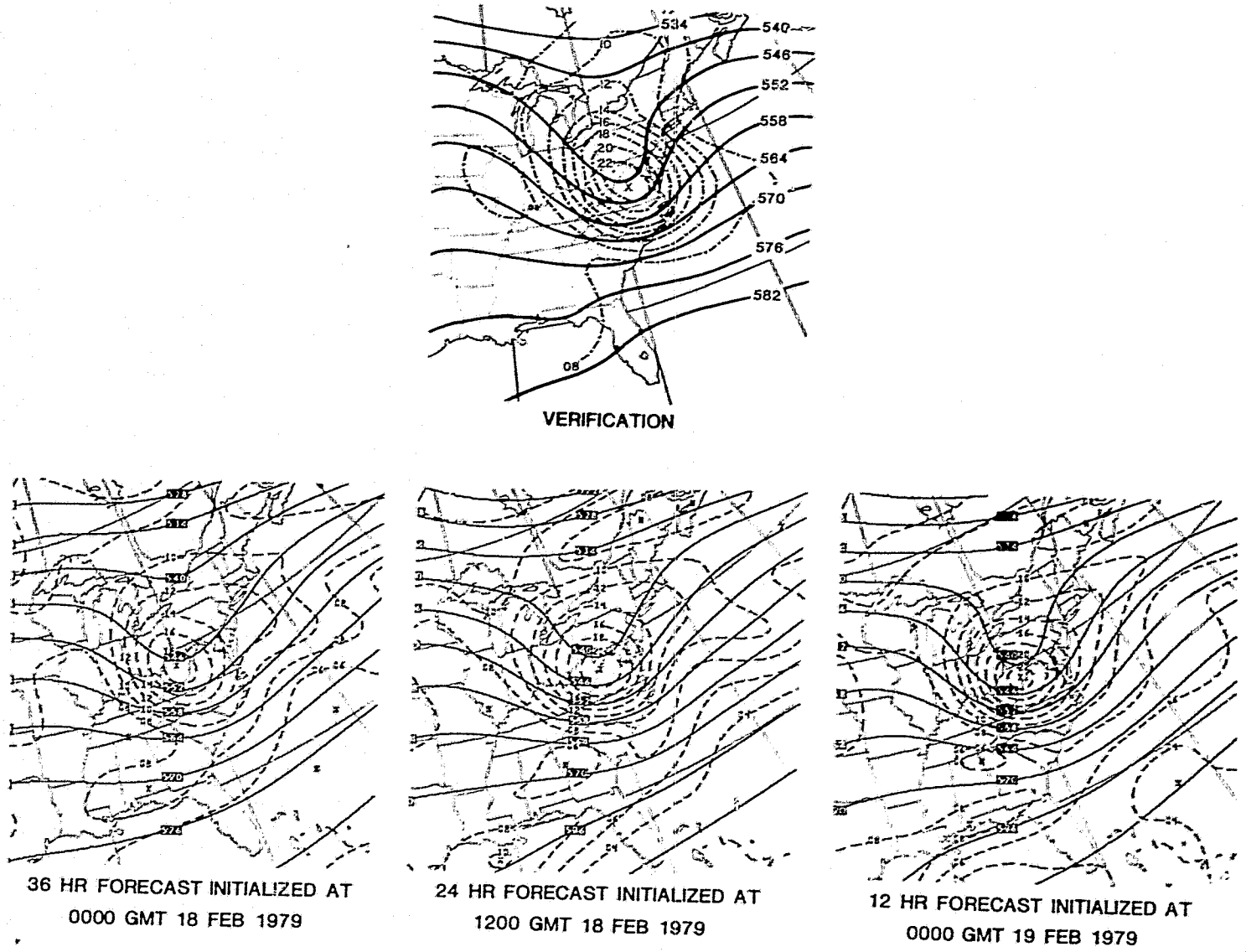

Figure 18. Comparison between the observed 500 mb geopotential height (solid, 540 = 5400 m) and absolute vorticity (dashed, 20 = 20 * $10^{-5}s^{-1}$) analysis (top) with three LFM–II forecast analyses (bottom) initialized prior to 1200 GMT 19 February 1979.

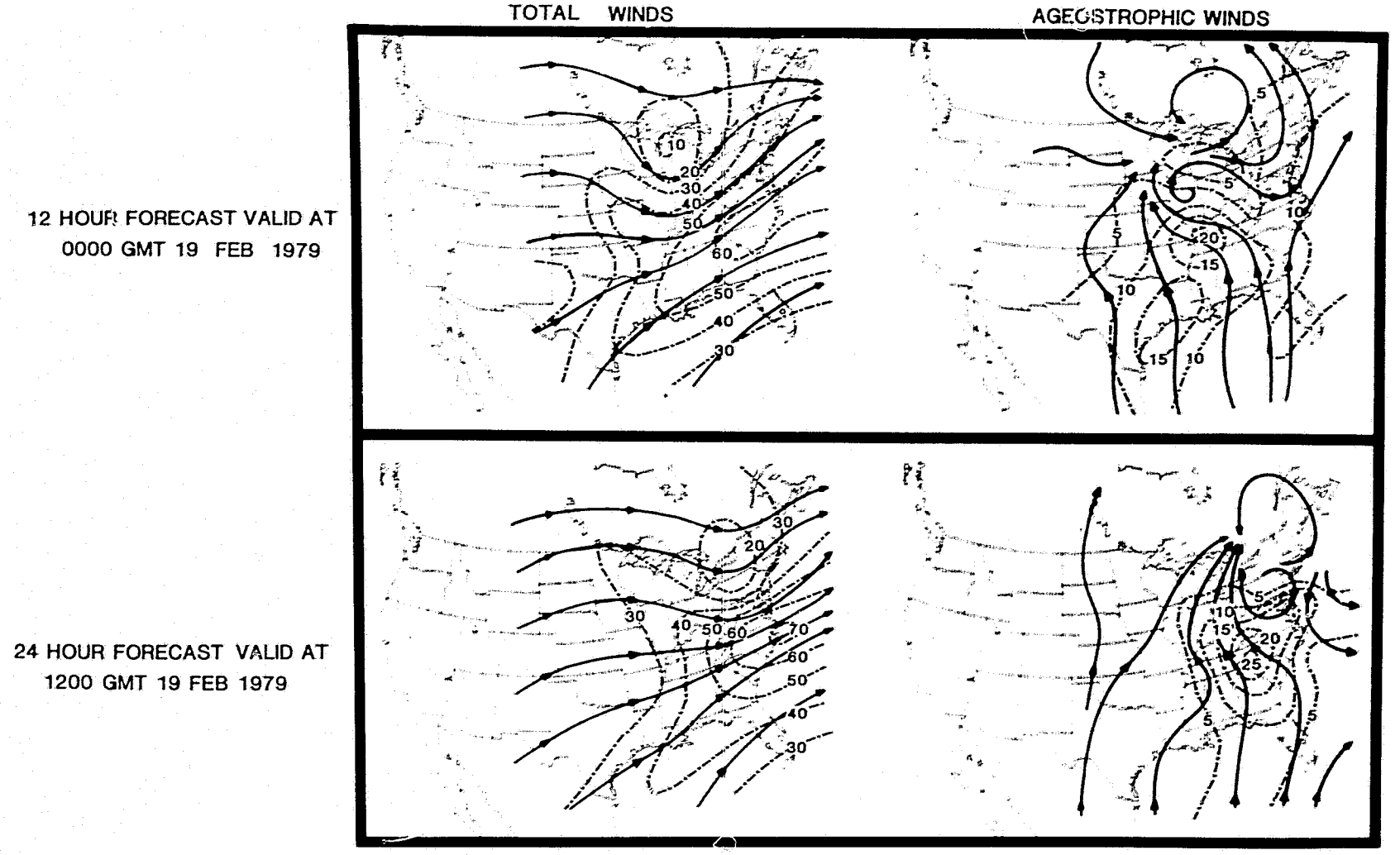

Figure 19. Twelve and 24-hour LFM-II forecasts of 300 mb total and ageostrophic winds initialized at 1200 GMT 18 February 1979. Solid lines indicate streamlines and dashed lines represent isotachs (ms^{-1}).

of the total and ageostrophic wind fields over 6-hour intervals for all three forecasts revealed that the LFM-II consistently predicted the expected transverse ageostrophic wind components in the exit and entrance region of the polar jet associated with the second wave without noticeable oscillation or deviation. Yet the forecast of the location and intensity of the surface low by all three model runs failed rather remarkably (Figure 20). The analyzed 1200 GMT 19 February 1979 surface map reveals an intense 1004 mb low center near the Maryland - Virginia coastline. The 36-hour forecast initialized at 0000 GMT 18 February provides no evidence of a developing cyclone as the model predicts a weak inverted trough along the southeastern and mid-Atlantic coast. The 24- and 12-hour forecasts, initialized at 1200 GMT 18 February and 0000 GMT 19 February, respectively, did develop a closed cyclonic circulation, but several hundred kilometers to the south and east of the actual location. The model also failed to capture the rapid deepening of the surface low or the enhancement of the pressure gradient in the vicinity of the cyclone center, as discussed by Bosart (1980).

Model Simulation of the LLJ

An apparent weakness in all three of the model simulations is the lack of a lower tropospheric thermal ridge, which developed along the East Coast in conjunction with the formation of the coastal front on 18 February and which provided a favorable environment for rapid cyclogenesis. Bosart (1980) has noted that significant sensible heat fluxes, which may be important for establishing the lower tropospheric thermal ridge, could not be properly accounted for within the model. A question that arises, however, is to what extent did the LFM simulate the development of the LLJ and the attending moisture and thermal advections along the Southeast coast during the pre-cyclogenetic period on February 18?

Figure 21 illustrates the 850 mb total and ageostrophic wind components for the 12h and 24h forecasts initialized at 0000 GMT 18 February. The LFM-II forecast the development of an LLJ over the Appalachian Mountains in eastern Tennessee at 12h into the forecast, and over West Virginia at 24h. These locations of the LLJ are several hundred kilometers north and west of

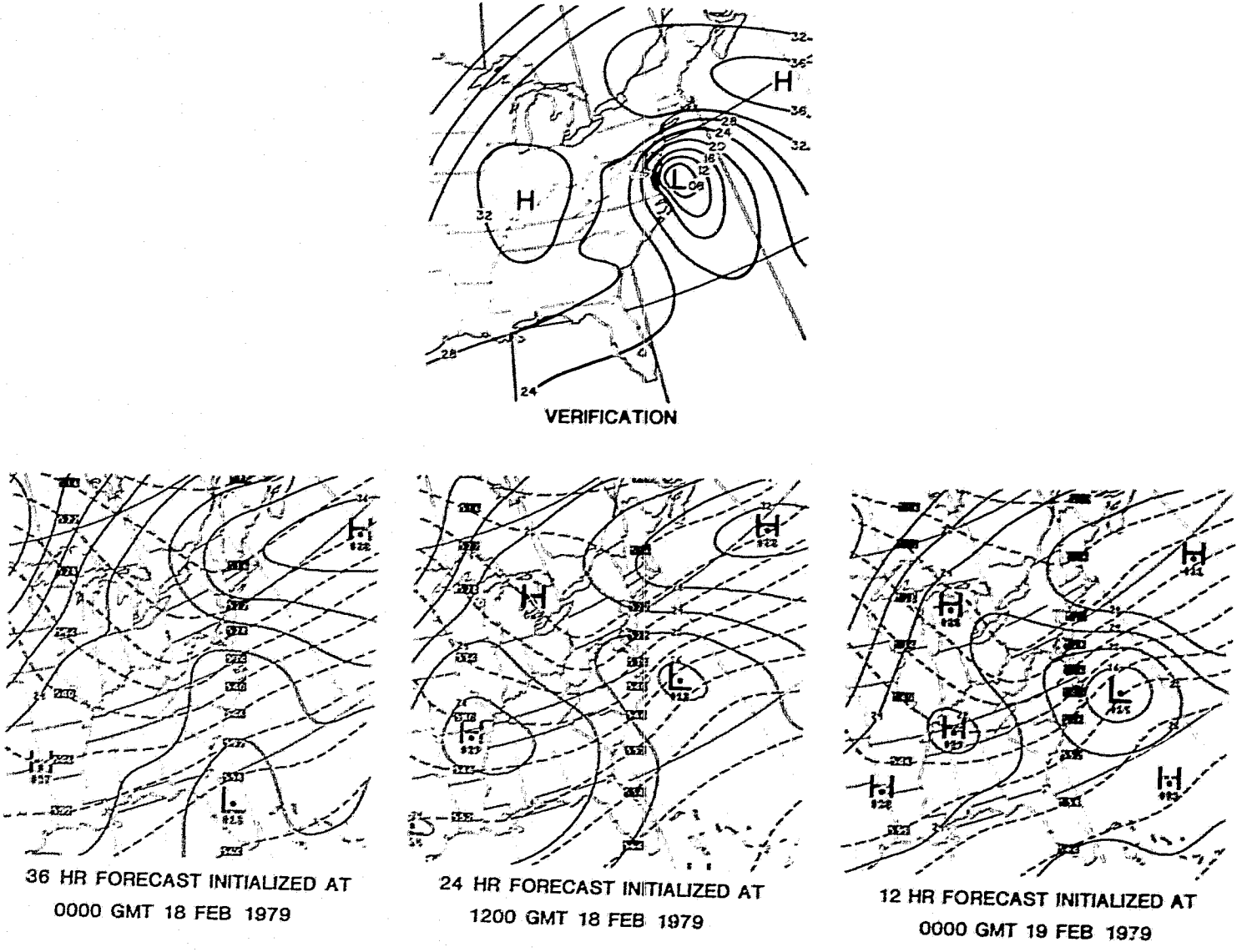

Figure 20. Comparison of 1200 GMT 19 February 1979 surface isobaric analysis (top: isobars are solid, 20 = 1020 mb) with three LFM-II forecast surface analyses (bottom: isobars are solid) and thickness analyses (dashed, 540 = 5400 m) initialized prior to 1200 GMT 19 February 1979.

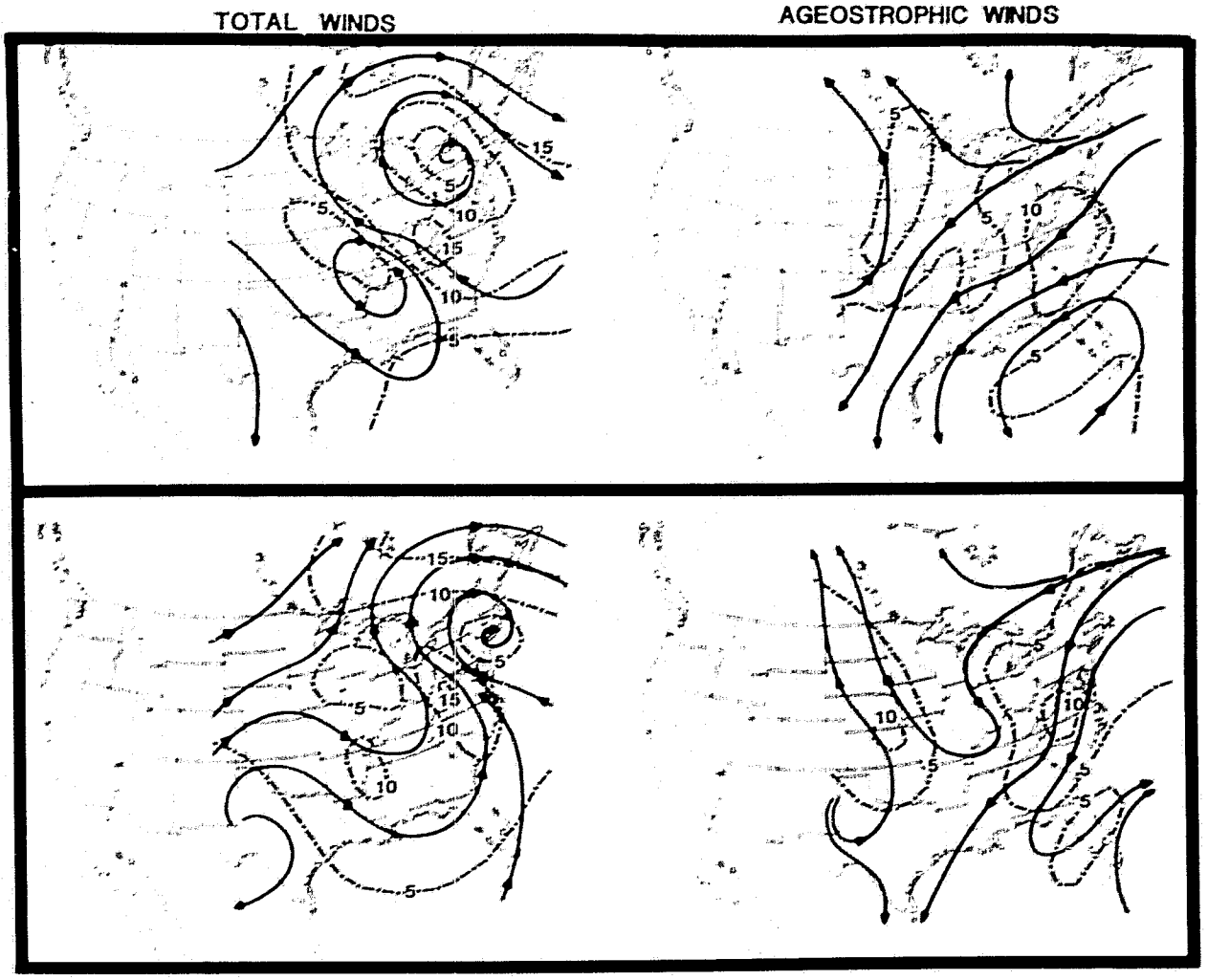

Figure 21. Twelve- and 24-hour LFM-II forecasts of 850mb total and ageostrophic winds initialized at 0000 GMT 18 February 1979. Solid lines indicate streamlines and dashed lines represent isotachs (ms^{-1}).

the coastal regions where the low level wind maxima were actually observed (Figures 3 and 10). The 12h and 24h forecasts for the ageostrophic wind reveal an east-northeasterly flow and not the south-southeasterly direction that was diagnosed near the 850mb level on the 292k surface. The highly ageostrophic LLJ that developed immediately along the East Coast was not forecast by any of the LFM-II model simulations reviewed for this analysis.

The 850mb isallobaric winds were computed using the LFM-II geopotential height tendencies measured over 12h periods ending at 1200 GMT 18 February and 0000 GMT 19 February (Figure 22). The most striking feature is that the LFM isallobaric fields significantly lag the observed analyses (Figure 17) by as much as 12 hours. At 1200 GMT 18 February the model has very weak isallobaric flow along the coast and significant east-southeast isallobaric winds located well to the west of the coastal region where the observed southeasterly isallobaric winds were maximized. It is not until the 12h period after 1200 GMT 18 February that the LFM generated significant isallobaric winds along the coast. However, even with this forcing, the ageostrophic wind remained north-northeasterly (Figure 21), rather than east-southeasterly as observed. Apparently, the northeasterly ageostrophic flow at the 850mb level in the LFM-II simulation (Figure 21) is heavily weighted toward the inertial-advective term in (1) associated with the strongly confluent southeasterly flow in the mid-Atlantic states. It, therefore, appears that the model simulations did not properly account for the isallobaric forcing of the LLJ along the East Coast as Discussed in Section 3.

Model Simulation of the Subtropical Jet and Associated Mass Adjustments

The next step in the examination of the LFM-II simulation is the model's forecast of the accelerating STJ that was linked to the development of the LLJ (see Section 3). Figure 23 illustrates the 12h and 24h LFM-II forecasts (initialized at 0000 GMT 18 February) of the total and ageostrophic 300mb winds. During the initial 12 hours of the forecast, the time during which the STJ accelerated to nearly 65 ms^{-1} at the 300mb level (Figure 3) and was observed to be

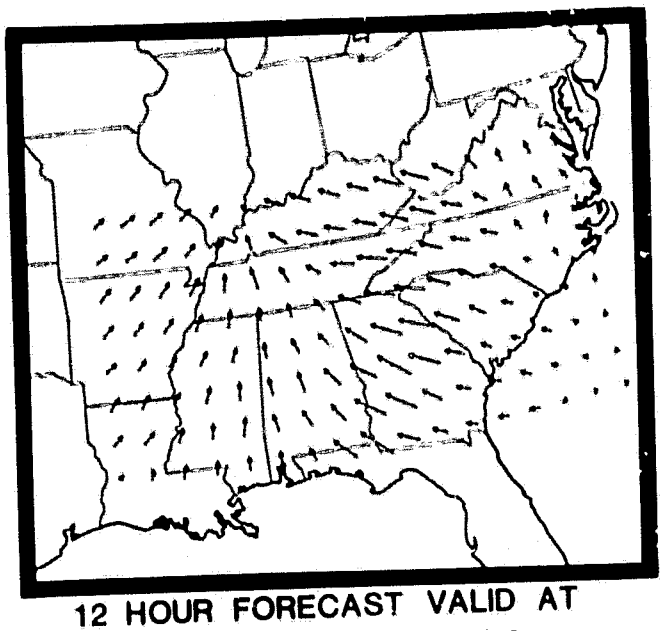

12 HOUR FORECAST VALID AT
1200 GMT 18 FEB 1979

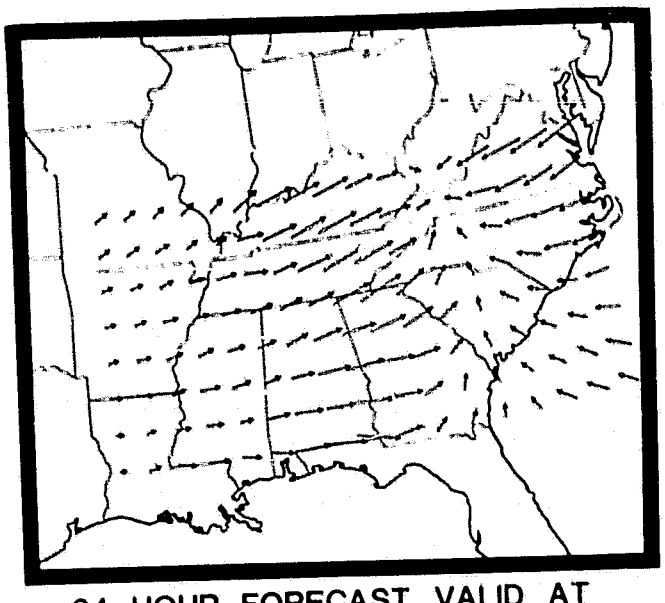

24 HOUR FORECAST VALID AT
0000 GMT 19 FEB 1979

0 5 10

Figure 22. 850 mb isallobaric winds generated from LFM-II forecast geopotential heights initialized at 0000 GMT 18 February 1979, using 12-hour ϕ tendencies. The magnitude (ms^{-1}) of the vectors are scaled at the bottom of the figure.

noticeably supergeostrophic, the LFM-II generated a 60 ms^{-1} jet streak, which was becoming increasingly supergeostrophic (by 20 ms^{-1}, Figure 23) in the exit region of a jet streak.

The forecast ageostrophic winds at the 300mb level are directed from the south along the entire axis of the STJ in conjunction with the accelerating nature of the flow and apparently in response to the strongly confluent flow into the polar jet streak located off the Northeast coast. It is not until 18h to 24h into the forecast period that the expected transverse ageostrophic pattern associated with the supergeostrophic streaks were diagnosed in this forecast (Figure 23). Figure 24 depicts the 3-hourly forecasts of the ageostrophic wind relative to the position of the subtropical jet streak from 0000 GMT 18 February to 0600 GMT 19 February. A slow oscillation of the ageostrophic winds in the exit regions of the jet streak exists from 0000 GMT 18 February 1979 to 1800 GMT 19 February 1979 as the ageostrophic wind vector veered from a southerly to a more northerly direction. By 24 hours into the forecast, the jet streak is absorbed into the current east of the Carolinas (Figure 20C), but a relative maximum still exists. By 30 hours the ageostrophic winds are once again southerly along the entire axis of the jet despite the presence of supergeostrophic flow.

Vertical cross sections of the model predicted potential temperature field were derived from grid points (Figure 25) nearest to the RAOB stations used for the analysis in Section 3 (Figure 16) to determine the extent to which the LFM-II properly simulated the mass adjustments near the STJ. The cross-sections from the LFM-II forecast initialized at 0000 GMT 18 February (Figure 26) illustrate two important features. First, the mass convergence to the right of the STJ (to the right of C in Figure 26) was not predicted by the LFM-II. The isentropes between the 200mb and 600mb levels were actually contracting rather than spreading apart. It is not until 18h into the model simulation that lower tropospheric isentropes are forced to higher pressure at points D and E at a time when the 300mb ageostrophic flow finally reversed to a more northerly direction (Figure 24). Second, rapid cooling in the boundary layer immediately to the left of D

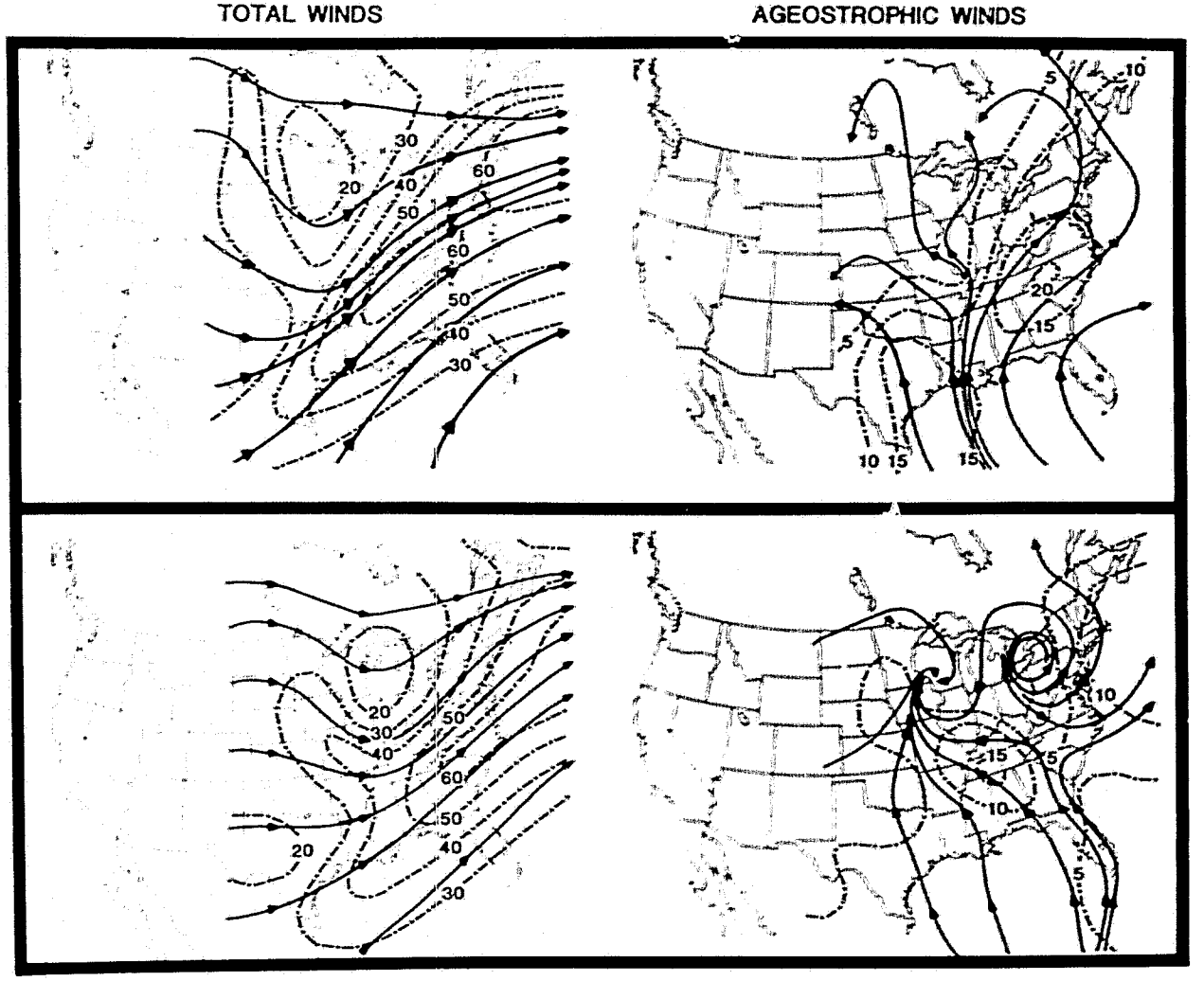

Figure 23. Twelve- and 24-hour LFM-II forecasts of 300 mb total and ageostrophic winds initialized at 0000 GMT 18 February 1979. Solid lines indicate streamlines and dashed lines represent isotachs (ms^{-1}).

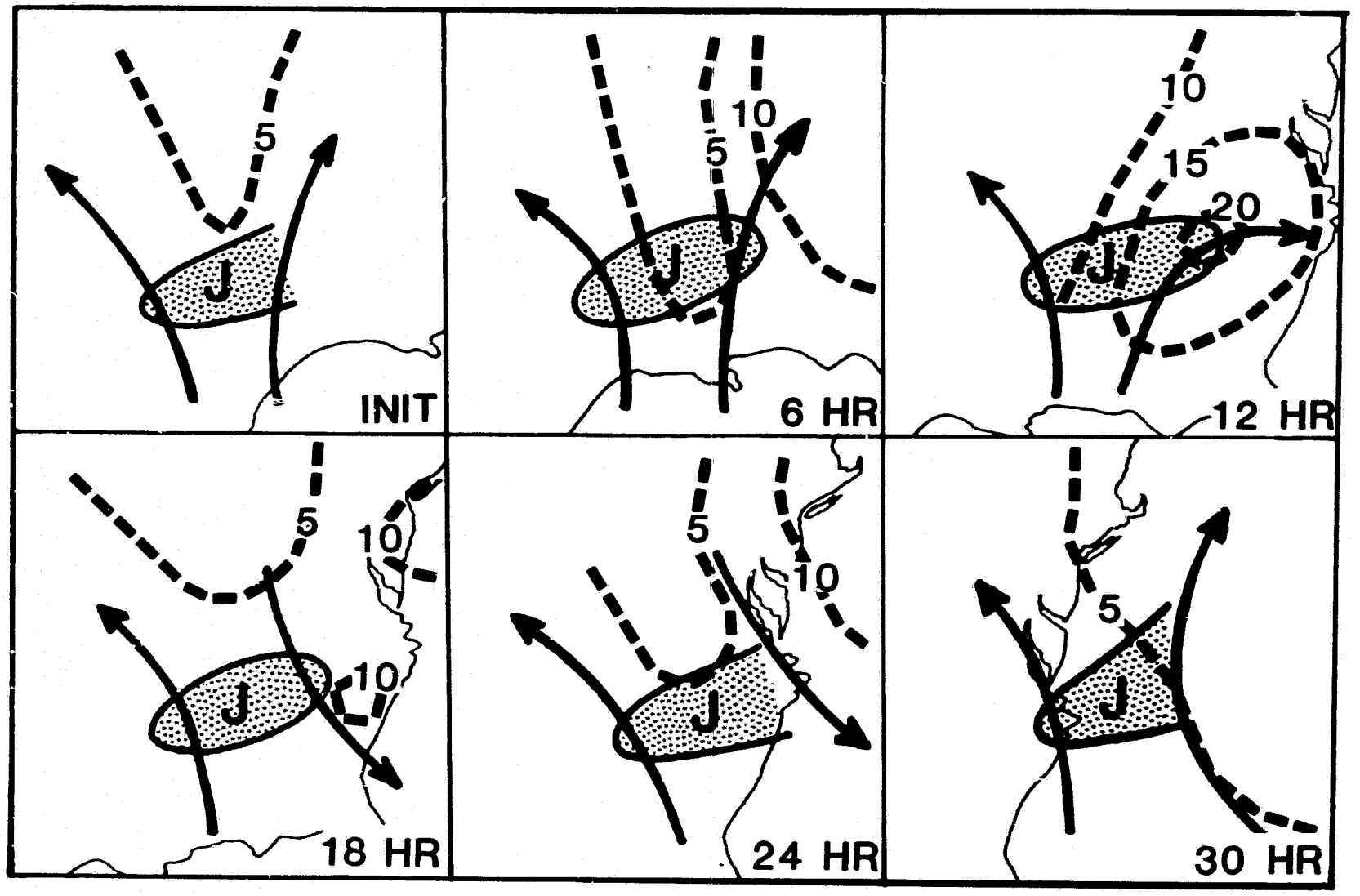

Figure 24. Six-hourly evolution of the LFM-II generated 300 mb jet streak [J represents location of velocity maximum; solid line surrounding shading represents winds greater than (60 ms^{-1})] and ageostrophic winds, where direction is indicated by arrows, and speed by isotachs (dashed, ms^{-1}) from LFM-II forecast initialized at 1200 GMT 18 February 1979.

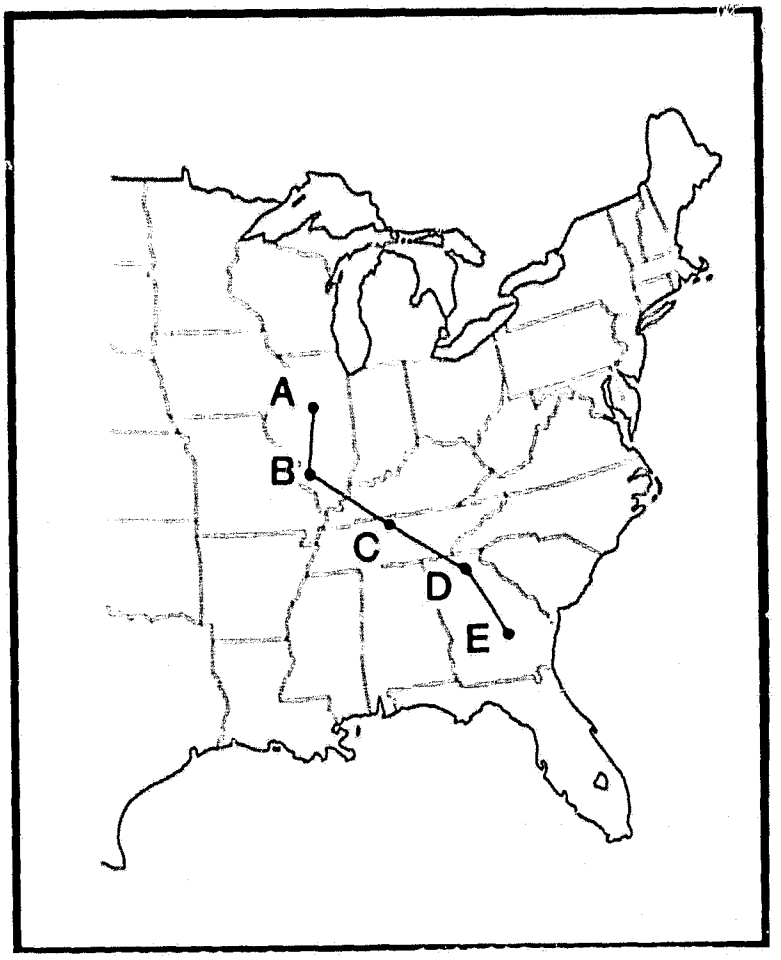

Figure 25. Points A through E represent locations of LFM generated cross section.

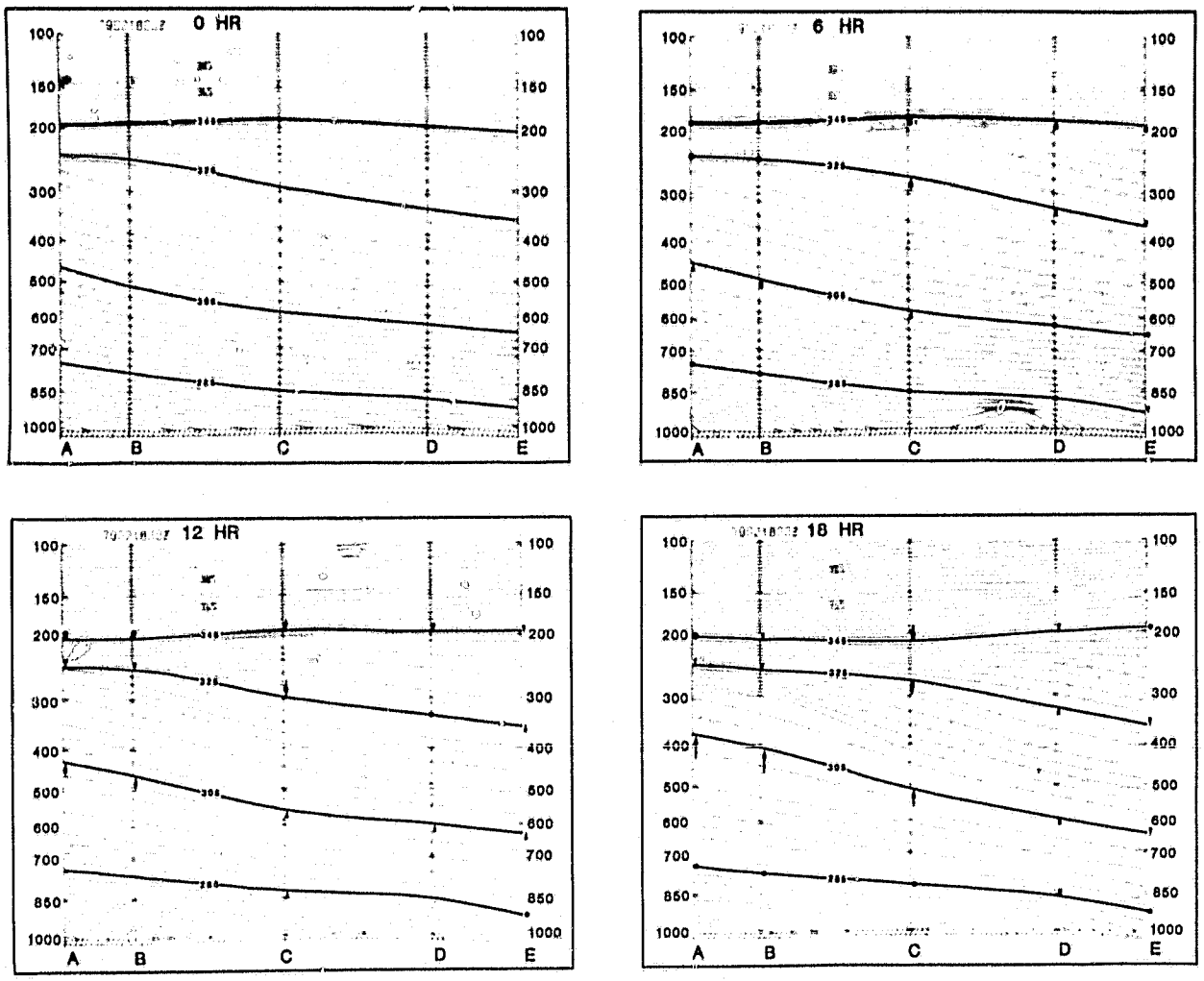

Figure 26. LFM-II generated cross sections of potential temperature, including initial analysis at 0000 GMT 18 February 1979 (top left) and 6-hourly forecasts ending at 1800 GMT 18 February 1979 (bottom right). Heavy lines represent 285°K, 305°K, 325°K and 345°K isentropes. Arrows reflect 6-hourly movement from previous time (end of arrow) to current time (arrow head).

at 6h and 12h is a manifestation of the damming effect near the Blue Ridge Mountains. It appears that the cold air is slightly west of the observed location, a displacement which is probably a function of the model terrain. The impact of this feature on the forecast was not pursued.

Summary of Model Diagnostics

Combining the information from the simulated 300mb flow (Figures 23 and 24), the 850mb analyses (Figures 21 and 22) indicates that the LFM-II predicted a direct circulation along the East Coast during the first 18h of the 0000 GMT 18 February simulation. A 300mb ageostrophic flow directed toward the cyclonic side of a complex jet flow is coupled with a persistent 850mb northerly ageostrophic flow along the entire East Coast, while isentropes contracted to the right of the STJ rather than apart as was observed. The model appears to be responding to the strongly confluent flow into the polar jet off the New England coast in maintaining the direct circulation during the first 18h of the model forecast. Since the forecast 850mb ageostrophic flow remains from the north, the model suppresses the development of the observed southeasterly LLJ. Hence, the strong thermal advection along the coast, which could have established the thermal ridge prior to cyclogenesis, would also be badly forecast.

It is not until 24h into the forecast that the upper level ageostrophic flow near the supergeostrophic STJ is reversed to the expected northerly component. It is also during this period that (1) the isallobaric center finally shifts to the Carolina coast (Figure 22), a full 12h after the observed center had already acted to generate a highly ageostrophic LLJ, and (2) an 850mb ageostrophic southerly wind has finally developed, but well to the southeast of the Carolina coast. However, the 300mb ageostrophic flow continues the rotation back to a southerly flow by 30h. Subsequent model simulations and LFM analyses all indicate that the 300mb ageostrophic winds are directed more toward the anticyclonic side of the STJ off the East Coast during the critical pre-cyclogenesis period. Yet the magnitude of this component remains small and appears to be more associated with the polar jet merging with the weakening STJ as depicted in Figure 19.

The analysis of the LFM-II presented in this report basically illustrates a poor prediction of the pre-cyclogenetic mass-momentum adjustments associated with the supergeostrophic subtropical jet and development of the LLJ off the East Coast. The model predicted a direct circulation along the East Coast during the period 0000 GMT 18 February to 0000 GMT 19 February and lagged in developing a lower tropospheric isallobaric forcing. The actual analysis emphasizes the existence of an indirect circulation with the LLJ forming along the Southeast coast immediately prior to cyclogenesis representing the lower branch of the indirect circulation. Subsequent model runs initiated at 1200 GMT 18 February and 0000 GMT 19 February develop weak indirect circulations along the East Coast, but it appears to be too little and too late to affect the environment in which the cyclone formed. None of the model forecasts develops the LLJ that was observed along the East Coast at three observing times.

The model analysis reveals that the LFM-II can be used to study jet streak circulations, which in turn, could be used for diagnosing potential model and initialization problems. The jet streak circulations are very sensitive to correctly specifying initial imbalances in the mass and momentum fields. It is possible that the oscillation in the ageostrophic component observed with the supergeostrophic STJ could have resulted from an initialization deficiency, a question that can only be addressed with more thorough numerical experiments.

5. CONCLUSIONS AND SUGGESTIONS FOR FUTURE RESEARCH

The analysis of the President's Day cyclone, 17-19 February 1979 reveals that a series of complex scale interactive processes is responsible for the development of the intense storm that produced heavy snowfall rates up to $12 cm h^{-1}$. Not only are large scale processes important for producing this storm, but mesoscale circulations also act to focus the adjustments associated with the initiation of the cyclone into a rather small area. It appears that the transverse circulations associated with jet streaks and coastal fronts act to produce a more favorable region for cyclogenesis and generate mesoscale regions of heavy snowfall through enhanced moisture transport and mechanical lift within the lower troposphere. These types of processes have been

previously discussed for establishing the conditions suitable for spring and summer convective storm systems (Uccellini and Johnson, 1979). However, the pre-cyclogenetic environment, with rapidly accelerating upper tropospheric flow, is far more complicated than the simplified view of jet streak adjustments presented by Uccellini and Johnson for the case involving straight jet streaks in a non-cyclogenetic period.

Specific findings derived from the analysis include:

1. Two systems were responsible for the heavy snow in the Southeast and along the East Coast. The first area of heavy snow was basically confined to the Southeast and was associated with a noticeably supergeostrophic subtropical jet streak. The second area of heavy snow that extended up the East Coast was related to a second wave propagating eastward from the Ohio Valley. The second wave and its attending polar jet streak concentrated vorticity and upper level divergence and appears to be an important factor in the initiation of the cyclone off the Virginia - Carolina coast.

2. The supergeostrophic STJ forced mass adjustments that appear to play a role in the rapid formation of an intense, highly ageostrophic low level jet 24 hours prior to cyclogenesis in a manner consistent with the coupling process described by Uccellini and Johnson (1979). The differences in this case, however, are that the STJ accelerates in a short period of time and appears to be supergeostrophic along its entire length. Therefore, mass adjustments associated with an indirect transverse circulation that would normally be found in the exit region of an upper level jet streak were analyzed, in this case, within an extended domain near the STJ for the 0000 GMT to 1200 GMT 18 February period. The pattern of the mass adjustments across the STJ closely resembles Rossby's (1939) analytic solution for adjustments necessary to restore a supergeostrophic current to a balanced state.

3. The damming of cold air to the east of the Appalachian Range (Richwein, 1980) also makes an important contribution to the development of the LLJ in this case. The entrenchment of cold air in northern Georgia magnified and focused the isallobaric response to the larger scale

mass adjustments between the Blue Ridge Mountains and Atlantic coast. The effect was to increase the magnitude and gradient of the Ψ tendency and to increase the isallobaric wind component in the lower troposphere during the period in which the LLJ rapidly developed.

4. The isallobaric forcing of the LLJ played a dual role in generating subsynoptic to mesoscale regions of moderate to heavy snowfall. The LLJ accelerated the moisture transport into the region of heaviest snow for three consecutive observing periods. The convergent nature of the isallobaric wind appears to also be important for providing the lift necessary for condensation and subsequent heavy snowfall. The circulation associated with the coastal front further enhanced precipitation rates immediately to the west of the front for two consecutive observing periods (Bosart, 1980).

5. The development of the LLJ could be an important factor in the development of the coastal front and lower tropospheric thermal ridge through shearing deformation and enhanced thermal advections, respectively. The evolution of these fields was a critical factor during the pre-cyclogenesis period that apparently primed the Virginia coast for the rapid cyclogenesis which occurred on 19 February.

6. As in Bosart's analysis (1980), the performance of the LFM-II model simulation is reviewed. Although the model does a credible job in simulating the Ohio Valley wave, which apparently initiates the rapid cyclogenesis, only a weak cyclone was predicted well to the southeast of the actual cyclone center. It appears that the model does not accurately simulate an indirect circulation for the noticeably supergeostrophic STJ on 18 February, but rather predicts a direct circulation in response to the confluent PFJ located in the Northeast. The consequence is the failure of the LFM to accurately predict (1) the isallobaric forcing depicted in the analysis, (2) the southeasterly ageostrophic flow along the coast, and (3) the development and evolution of the LLJ along the East Coast. Therefore, the mass-momentum adjustments, which could have established the thermal ridge off the East Coast and possibly aid the development of a coastal front during the pre-cyclogenetic period, were severely lacking in the model simulations.

Several important questions are left unanswered which deserve further research.

1. What caused the acceleration of the STJ? The concept that the magnitude of the STJ increases in response to an existing confluence zone (Namias and Clapp, 1949) may not readily apply in this case. While a confluence zone does exist over New Mexico and Mexico, the accelerations of the STJ seem to occur prior to or in conjunction with the increased confluence in the southern United States. Yet, the supergeostrophic nature of the flow prior to 0000 GMT 19 February indicates that the wind forced the mass to adjust rather than a local mass distribution forcing the wind to adjust. The acceleration of the STJ might also be linked to tropical convective regions that generate the persistent ageostrophic wind components which act to increase the magnitude of the STJ as described by Paegle et al. (1979). The FGGE data sets could be useful in resolving the possible global interaction for this case.

2. To what extent did the diabatic and boundary layer processes play a role in the development of the LLJ and the rapid cyclogenesis along the East Coast? This study emphasizes the adiabatic adjustments associated with the supergeostrophic STJ and development of the LLJ and the baroclinic nature of the Ohio Valley wave and its role in initiating cyclogenesis. Bosart's (1980) analysis tends to emphasize the diabatic and boundary layer processes in explaining the onset of cyclogenesis and rapid vortex formation. The lack of data precludes the detailed analysis necessary to determine the relative importance of these processes and therefore dictates the need for careful numerical experiments to resolve this problem.

3. What is the extent to which the reduced static stability off the coast plays a role not only in the development of the LLJ, but also in the rapid formation of the cyclonic circulation? Both the LLJ and the cyclone underwent explosive development as upper tropospheric waves and jet streaks approached the coast. Careful numerical experiments are needed to assess the extent to which reduced static stability in the lower troposphere influences the LLJ development and rapid cyclogenesis.

4. To what extent is the failure of the LFM-II model simulations a function of poor boundary layer representation (as emphasized by Bosart, 1980) or poor jet streak simulation with

respect to the STJ and LLJ (as discussed in this report)? While not minimizing the importance of the boundary layer for these types of storms, questions could be raised as to whether even a perfect representation of the boundary layer would reverse the transverse circulation along the East Coast in the LFM-II forecast from a direct to an indirect circulation. Model experiments are needed to determine the degree to which the jet streak simulations could be improved in the LFM-II. Experiments with various initialization techniques are also needed to specifically determine if the oscillations in the ageostrophic flow near the STJ are a function of an improper balance of forces within the initialized mass and momentum fields or if the oscillations are real but out of phase.

The interactions of tropical-extratropical regimes associated with the subtropical and polar jets, the upper-lower tropospheric coupling associated with the development of the LLJ, the terrain modification due to the damming effect, and the complex baroclinic processes associated with the initiation of the cyclone by the second wave and polar jet streak all combined to produce the rapid cyclogenesis that marked the President's Day cyclone. These complex interactions suggest that global to synoptic to mesoscale cascade processes will need to be resolved to properly simulate this type of storm. The meso-synoptic-global interactions are also important as the cyclone evolved from the phasing of two mesoscale, isallobaric centers and rapidly grew into a vortex which ultimately changed the large scale circulation over the Atlantic Ocean. It will take a combined diagnostic-numerical model approach to resolve the interesting questions and problems related to the analysis of the President's Day cyclone.

Acknowledgements

We greatfully acknowledge the following people who have aided in our analysis and report of the President's Day cyclone: Dr. Dennis Deaven of NMC for providing the tapes of the LFM-II; Mr. Thomas Whittaker, Ron Sznaider and Richard Seline of the Space Science and Engineering Center (SSEC) at the University of Wisconsin for their assistance with processing the RAOB data on the SSEC McIDAS used in the isentropic analysis and processing the LFM model output used

in Section 4; Mr. Andrew Horvitz of NESS for assembling the SMS-GOES infrared imagery for our use and Mrs. Paula Boucher for typing the many drafts of the manuscript. Discussions with participants of the second Cyclone Workshop and with Dr. Robert Atlas and Dr. Wayman Baker of GLAS regarding this case were useful in shaping the final version of this report. This work was supported in part by the National Science Foundation (NSF Grant 7722976).

6. REFERENCES

Bosart, L. F., 1980: The President's Day Snowstorm of 18-19 February 1979: A Sub-synoptic scale event. Manuscript submitted to Mon. Wea. Rev.

Bosart, L. F., 1975: New England coastal frontogenesis. Quart. J. Roy. Meteor. Soc., 101, 957-978.

_____, C. J. Vaudo, and J. H. Helsdon, Jr., 1972: Coastal frontogenesis. J. Appl. Meteor., 11, 1236-1258.

Cahn, A., 1945: An investigation of the free oscillations of a simple current system. J. Meteor., 2, 113-119.

Carlson, T. N., 1980: Airflow through midlatitude cyclones and the comma cloud pattern. Mon Wea. Rev., 108, 1498-1509.

Foster, J. L., and R. J. Leffler, 1979: The extreme weather of February 1979 in the Baltimore-Washington area. Nat. Wea. Dig., 4, 16-21.

Marks, F. D., and P. M. Austin, 1979: Effects of the New England coastal front on the distribution of precipitation. Mon. Wea. Rev., 107, 53-67.

Namias, J., and P. F. Clapp, 1949: Confluence theory of the high tropospheric jet stream. J. Meteor., 6, 330-336.

Paegle, J., J. E. Paegle, F. P. Lewis and A. J. McGlasson, 1979: Description and interpretation of planetary flow structure of the winter 1976 DST data. Mon. Wea. Rev., 107, 1506-1514.

Richwein, B. A., 1980: The damming effect of the southern Appalachians. Nat. Wea. Dig., 5, 2-12.

Rossby, C. G., 1938: On the mutual adjustment of pressure and velocity distributions in certain simple current systems II. J. Mar. Res., 7, 239-263.

Shapiro, M. A., 1970: On the applicability of the geostrophic approximation of upper-level frontal-scale motions. J. Atmos. Sci., 27, 408-420.

Schwerdtfeger, W. E., 1973: Mountain Barrier Effect on the Flow of Stable Air North of the Brooks Range. Climate of the Arctic, 204-208.

Uccellini, L. W., 1976: Operational diagnostic applications of isentropic analysis. Nat. Wea. Dig., 1.

_____, and D. R. Johnson, 1979: The coupling of upper and lower tropospheric jet streaks and implications for the development of severe convective storms. Mon. Wea. Rev., 107, 682-703.

_____, 1980: On the role of upper tropospheric jet streaks lee side cyclogenesis in the development of low level jets in the Great Plains. To appear in Mon. Wea. Rev., October 1980.

Weber, E. M., 1980: Merging height fall centers-two examples. Nat. Wea. Dig., 5, 13-17.

APPENDIX

NMC MODEL POSTPROCESSING PROCEDURES

This appendix summarizes the procedures used by NMC to post-process their model forecast fields for general use. Both NMC operational fine and coarse mesh models are formulated in sigma coordinates. Thus, all forecast variables must be interpolated from the sigma framework to mandatory pressure levels. This is accomplished with the assumption that the vertical variation of dependent variables is linear with respect to p. The variables are not interpolated across the tropopause except for geopotential height. If a mandatory pressure surface is located just above (below) the tropopause, parameters are determined by extrapolation down from the two stratospheric layers (upward from the two upper tropospheric layers).

After interpolation to pressure levels, the model data are filtered to damp unrealistic high frequency waves in the solution. The smoothing involves single passes by three different filters. Since the filters are symmetric, only the weights for the upper left quadrant are presented. The filters, in order of application are:

1. a 9-point smoother,

1/16	1/8
1/8	1/4

2. a 9-point desmoother,

1/16	-3/8
-3/8	9/4

3. a 49-point smoother

1/1024	0	-9/1024	-16/1024
0	0	0	0
-9/1024	0	81/1024	144/1024
-16/1024	0	144/1024	256/1024

Near the boundaries the array is collapsed to smaller size. The spectral responses of the 49-point smoother and the combined application of the three filters are presented in NOAA Technical Procedures Bulletin #174. An interpolation of the model data to the NMC display grid also involves further smoothing of the model fields.

The LFM, due to its limited domain, possesses a tendency to exhibit a trapped, large-scale, predominantly external gravity wave. A "deslosh" routine is used by NMC to eliminate this wave from the LFM forecast geopotential fields. A 500 mb geopotential is calculated by relaxation from the non-divergent 500 mb forecast wind components. The difference between the wind-derived geopotential and the predicted 500 mb geopotential is subtracted from the geopotential at other mandatory levels. This procedure does not modify the model thickness values. The resultant geopotential heights are then filtered as discussed earlier.

The vertical motion omega is also determined during post-processing for the mandatory pressure levels. Omega is calculated for the midpoint of each σ-layer at every second time step during the 2 hours preceding every 6-hour archive (hours 6, 12, 18, 24, etc.) from its expansion in sigma coordinates given by

$$\omega(x, y, \sigma, t) = \frac{dp}{dt} = \frac{\partial p}{\partial t_\sigma} + \underset{\sim}{U} \cdot \nabla_\sigma p + \dot{\sigma} \frac{\partial p}{\partial \sigma}. \qquad \text{(A-1)}$$

The average value over the two-hour period is then interpolated to mandatory pressure levels.